On the computation of reproduction numbers for the environment-host-environment cholera transmission dynamics

January 2, 2020

Antonella Lupica[a,b1], Abba B. Gumel[c,d2] and Annunziata Palumbo[b3]

[a] *Department of Mathematics and Computer Sciences, University of Catania, V.le A. Doria 6, 95125 Catania, Italy.*

[b] *Department of Mathematical and Computer Sciences, Physical Sciences and Earth Sciences, University of Messina, V.le F. D'Alcontres 31, 98166 Messina, Italy.*

[c] *School of Mathematical and Statistical Sciences, Arizona State University, Tempe, Arizona, USA.*

[d] *Other affiliation: Department of Mathematics and Applied Mathematics, University of Pretoria, Pretoria 0002, South Africa.*

Abstract

This study presents a new model for the environment-host-environment transmission dynamics of *V. cholerae* in a community with an interconnected aquatic pond-river water network. For the case when the human host is the sole target of anti-cholera control and the volume of water in the pond is maximum, the disease-free equilibrium of the model is shown to be globally-asymptotically stable whenever a certain epidemiological threshold, known as the basic reproduction number ($\mathcal{R}_0$), is less than unity. The epidemiological implication of this result is that cholera can be eliminated from the community if the control strategies implemented can bring (and maintain) $\mathcal{R}_0$ to a value less than unity. Four scenarios, that represent different interpretations of the role of the *V. cholerea* pathogen within the environment, were studied. The corresponding basic reproduction numbers were shown to exhibit the same threshold property with respect to the value unity (i.e., if one is less (equal, greater) than unity, then the three others are also less (equal, greater) than unity. Further, it was shown that for the case where anti-cholera control is focused on the human host population, the associated type reproduction number of the model (corresponding to each of the four transmission scenarios considered) is unique. The implication of this result is that the estimate of the effort needed for disease elimination (i.e., the required herd immunity threshold) is unique, regardless of which of the four transmission scenarios is considered. However, when any of the other two bacterial population types in the aquatic environment (i.e., bacterial in the pond or river) is the focus of the control efforts, this study shows that the associated type reproduction number is not unique. Extensive numerical simulations of the model, using a realistic set of parameters from the published literature, show that the community-wide implementation of a strategy that focus on improved water quality, sanitation and hygiene (known as WASH-only strategy), using the current estimated coverage of 50% and efficacy of 60%, is unable to lead to the elimination of the disease. Such elimination

[1]Corresponding author: Email: *alupica@unime.it*

[2]Email: *agumel@asu.edu*

[3]Email: *apalumbo@unime.it*

is attainable if the coverage and efficacy are increased ((e.g., to 80% and 90%, respectively). Further, elimination can be achieved using a strategy that focus on oral rehydration therapy and the use of antibiotics to treat infected humans (i.e., treatment-only strategy) for moderate effectiveness and coverage levels. The combined hybrid WASH-treatment strategy provides far better population-level impact *vis a vis* disease elimination. This study ranks the three intervention in the following order of population-level effectiveness: combined WASH-treatment, followed by treatment-only and then WASH-only strategy.

Keywords: *V.cholerae*; type reproduction number; asymptotic stability; transmission scenarios; pond-river water network.

1 Introduction

Cholera, a bacterial disease that affects the intestinal track, is caused by the bacterium *Vibrio cholerae*. Infection with the disease, which can be effectively treated using antibiotics if caught early (typically within the first two days of onset of symptoms), can result in severe diarrhoea and (subsequently) dehydration, which, if untreated, can be fatal. Cholera continues to be a major public health problem in many parts of the world (most notably in the Indian sub-continent and some parts of Africa, Asia and Latin America) [1, 44, 45, 47] (Figure 1). Figures from the World Health Organization (WHO) [45] show that, each year, the disease accounts for between [1.3- 4] million cases and [21.000-143.000] fatalities globally. It is noteworthy that many cholera-endemic countries are now pledging to end cholera outbreaks by 2030 [44].

Although a secondary human-to-human mode of cholera transmission exist [28, 56, 63], cholera is primarily transmitted to humans from the environment by ingesting food or water contaminated with the bacterium *V. cholerae* [17, 29]. The disease has a short incubation period (ranging from a few hours to five days [55]) and its common symptoms are diarrhoea (leading to severe dehydration), vomiting, loss of skin elasticity, thirst, and muscle cramps [55, 69]. Most cholera-infected people (at least 80%) do not become ill, although they may carry the *V. cholerae* bacterium for weeks and slowly excreting it into the water supply [6, 55, 45]. However, when illness does occur, about 80%-90% of episodes are of mild or moderate severity and are difficult to distinguish clinically from other types of acute diarrhoea [45].

Basic preventive measures, such as improvements in sanitation systems, effective and adequate drinking water and sewage treatment, and improved food and personal hygiene, are generally adopted in cholera-endemic areas to minimize human contact with *V. cholorae*-contaminated sources. In particular, the water, sanitation and hygiene (WASH) strategy is widely implemented in endemic areas [26]. The disease can be successfully treated, in most cases, using oral rehydration therapy [68, 48] (which is highly effective, safe, and simple to administer) and antibiotics [36, 53, 68, 48]. Owing to the common and widespread administration of antibiotics to treat cholera-infected humans, the emergence of antibiotic resistant strains of *V. cholerae* is very well documented in the literature [35, 36, 55]. Furthermore, a number of safe and effective anti-cholera vaccines have been developed for use in humans (see, for instance, Safi et al. [27, 55] and some of the references therein). People infected with *V. cholerae* are generally treated using fluid replacement therapy and antibiotics [55, 56]. Cholera-endemic regions around the world that do not adhere to the aforementioned preventive measures, and provide access to treatment to infected people, continue to experience cholera outbreaks [1, 44, 45, 47].

Mathematical models, typically of the form of deterministic system of nonlinear differential equations, have been used to gain insight into the transmission dynamics and control of cholera in endemic areas. For instance, Capasso and Paveri-Fontana [13] developed the earliest model to describe the 1973 cholera epidemic in Bari, Italy [4]. Codeço [16] extended the two-dimensional model developed by Capasso and Paveri-Fortana to include the dynamics of the susceptible population. More recently, Pascual et al. [49] reviewed some quantitative facts about cholera and climate. In a short section, they proposed a model with four variables, i.e. the number of susceptible individuals, the number of infected individuals, the number

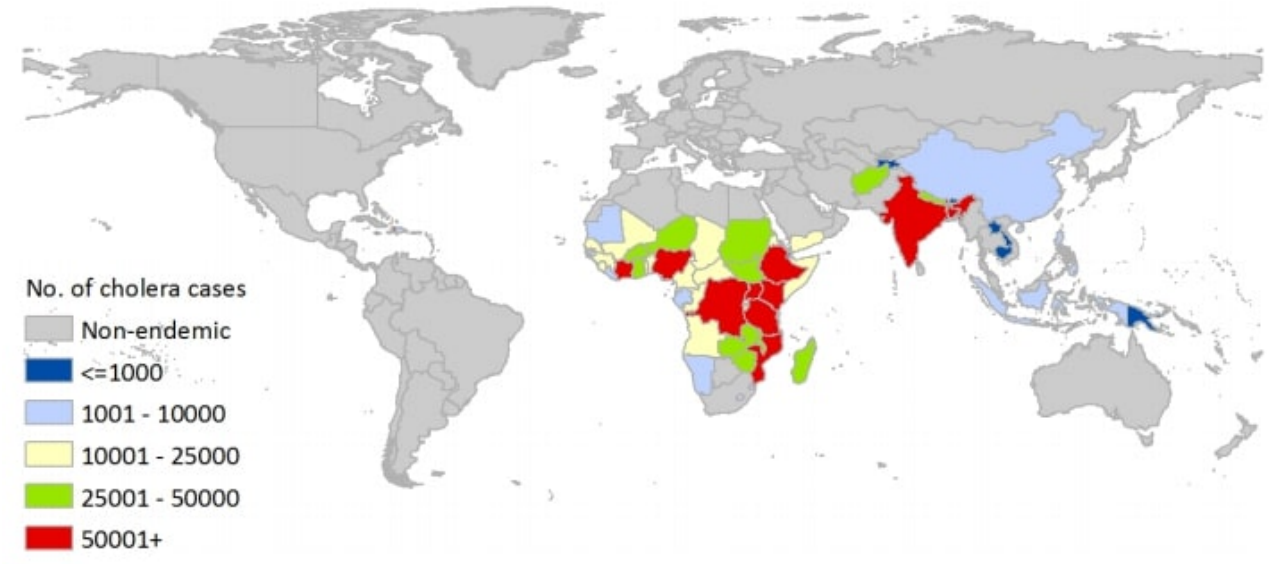

(a)

Figure 1: Global cholera map: geographical patterns of annual number of cholera cases in endemic countries. [1].

of fomites (or bacterial abundance) and the water volume. Further, authors in [7, 8, 9, 10, 15, 41] explored the problem of the spread of cholera, considering two or more populations of bacteria living in two different but connected aquatic environments. Safi et al. [55] developed an 11-dimensional deterministic model for assessing the combined impact of dose-structured cholera vaccination and treatment on the dynamics of two cholera strains in a population.

The dynamics of the models developed for cholera transmission dynamics and control are generally governed by an epidemiological threshold, known as the *reproduction number* (and generally denoted by $\mathcal{R}_0$). Epidemiologically-speaking, the quantity $\mathcal{R}_0$ measures the average number of secondary infections generated by a typical infectious individual introduced into a completely susceptible population [2, 31]. In general, the disease dies out when $\mathcal{R}_0 < 1$ and persists in the population when $\mathcal{R}_0 > 1$. The *next generation operator method* (NGM), developed by Diekmann et al. [23, 22] and elaborated by van den Driessche and Watmough [66], is popularly-used in the mathematical biology community to compute this epidemiological quantity.

As noted by van den Driessche and Watmough [66], owing to the fact that cholera is an environment-host-environment epidemic, different expressions for $\mathcal{R}_0$ can be obtained, depending on the interpretation of the role of the environment. For example, Bani-Yaghoub et al. [5] highlighted the issue of calculating a valid expression for $\mathcal{R}_0$ for diseases transmitting through the contaminated environment. This problem, of computing the correct $\mathcal{R}_0$ for environmentally-transmitted diseases, can be overcome by using the notion of *type* reproduction numbers [30, 52], which provides a unique threshold value, regardless of the interpretations of the role of the environment.The concept of type reproduction number was further generalized by Shuai et al. [58, 59], useful when the control strategies act on a part of the population or on the interactions between the different populations.

The dynamics of cholera is greatly associated with environmental contamination (it is well-known that the bacterium is autochthonous to the aquatic environment [17]). In particular, *V. cholerae* inhabits seas, estuaries, brackish waters, rivers, and ponds of coastal areas of the tropical world [18, 43] (and surface water in proximity to cholera-infected individuals is frequently contaminated with the *V. cholerae* agent [61]). Further, the bacterium can survive long-term, perhaps for years, in such aquatic environments [17].

Hence, models for the transmission dynamics of the disease should incorporate the highly significant role such environmental factors play in the disease dynamics (vis a vis the production and long-term survival of *V. chlorea* in the aquatic habitat). Consequently, the aim of this study is to propose a new model for cholera transmission dynamics that take into account the role of environmental factors on the disease dynamics in addition to explicitly accounting for the impact of the hydrological fluctuations of the volume of available drinking water in a cholera-endemic setting. In particular, a cholera-endemic community with a local pond-river network as its source (reservoir) of available drinking water will be considered. The notion of the type reproduction number will be used to assess the population-level impact of various anti-cholera control strategies.

The paper is organized as follows. The model is formulated in Section 2. Its basic qualitative properties are also explored. Detailed computation of the basic reproduction numbers of the model, for all possible transmission scenarios, is reported in Section 3. The associated types reproduction numbers of the model are computed in Section 4. The developed model is used to assess the population-level impact of various anti-cholera control strategies are carried out in Section 5.

2 Formulation of Mathematical Model

The model to be designed in this study is built on two basic components, namely an epidemiology component for the disease dynamics in a human population and a hydrology component for the water balance (within the local pond-river system) . Cholera is endemic in many countries in Africa and Asia (mainly in India and Bangladesh), although a number of outbreaks have also occurred in Eastern Europe and Haiti. In most of the rural areas of these countries, drinking water supply source (and reserve) mostly comes from ponds and small rivers that are often interconnected [50]. Thus, cholera dynamics in such settings is associated with the contamination of the two local water sources with *V. cholerae* (i.e., cholera *ecology*), the inflow and outflow of water to and from the two interconnected water sources (i.e., water balance or *hydrology*), and *V. cholerae* transmission between humans due to human contact with the contaminated water sources (i.e., cholera *epidemiology*). The model we propose for this setting, which focuses on the primary mode of cholera transmission, captures the three main elements (of ecology, epidemiology and hydrology). In particular, the ecology-epidemiology-hydrology model to be designed in this study is that of the transmission dynamics of cholera in a cholera-endemic community whose main source of drinking water is a local network of a pond (typically defined as a small basin consisting of stagnant water) and a river (consisting of flowing water). Figure 2 depicts a schematic of a pond-river water network system for a typical cholera-endemic community.

The total human population at time t, denoted by $N(t)$, is split into mutually-exclusive compartments of susceptible ($S(t)$) and infected ($I(t)$) individuals, so that $N(t) = S(t) + I(t)$. Similarly, the total volume of water available to the community is split into the volume of water in the local pond (denoted by $V_p(t) > 0$) and the volume of water in the river ($V_r^* > 0$, assumed constant). Consequently, following [7, 8, 9, 10, 15, 41], the total *V. cholerae* bacteria population in the community at time t, is split into the total number of bacteria in the pond (denoted by $B_p(t)$) and the total concentration of *V. cholerae* bacteria in the river ($B_r(t)$). While it is assumed that the water volume in the river is constant, the water volume in the pond is assumed to vary with time (as this is affected by rainfall, evaporation and/or drainage [10, 15, 51]).
The population of susceptible humans is increased by recruitment (due to birth or immigration) at a *per capita* rate Π and by the recover from cholera infection at a rate γ^*. This population is decreased following the acquisition of cholera infection from the cholera-contaminated pond at a rate $\beta_p^* \dfrac{B_p}{k_p^* V_p + B_p}$, where β_p^* is the rate of cholera infection from a pond and k_p^* is the minimum concentration of *V. cholerae* in the pond that guarantees 50% chance of *V. cholerae* transmission per contact [49]. Similarly, infection is acquired from

(a) (b)

Figure 2: A pond-river network in a typical cholera-endemic setting. Figure 2(a) was adapted from [62], while Figure 2(b) was adapted from [64].

the (contaminated) river reservoir at a rate $\beta_r^* \dfrac{B_r}{k_r + B_r}$, where β_r^* is the infection rate and k_r is the saturation parameter that accounts for the minimum *V. cholerae* concentration in the river that guarantees 50% chance of cholera transmission. It is assumed that humans in all epidemiological compartments die naturally at a rate μ^*. Thus (where a dot represents differentiation with respect to time t):

$$\dot{S} = \Pi + \gamma^* I - \left(\beta_p^* \frac{B_p}{k_p^* V_p + B_p} + \beta_r^* \frac{B_r}{k_r + B_r} \right) S - \mu^* S.$$

The population of infected individuals is generated by the acquisition of infection from the pond or the river. It is decreased by recovery (at the rate γ^*), natural death (at the rate μ^*) and cholera-induced mortality at a rate δ^*. Hence,

$$\dot{I} = \left(\beta_p^* \frac{B_p}{k_p^* V_p + B_p} + \beta_r^* \frac{B_r}{k_r + B_r} \right) S - (\gamma^* + \mu^* + \delta^*) I.$$

It follows from the above two equations that the rate of change of the total human is given by:

$$\dot{N} = \Pi - \mu^* N - \delta I.$$

It is worth noting that, in the above formulation, the Michales-Menten (Holling type-II) incidence function is used to model the cholera transmission rates above.

The bacterial population in the pond is increased by *V. cholerae* shedding by infected humans at a rate θ_p^* and by the natural reproduction of free-living *V. cholerae* bacteria in the pond at the logistic rate $r \left(1 - \dfrac{B_p}{k_{bp}} \right)$ (where r is the reproduction rate and $k_{bp} > B_p(t)$ for all t is the carrying-capacity of free-living *V. cholerae* in the pond (i.e., k_{bp} is the maximal capacity of free-living bacteria in the environment)). This formulation is motivated by the fact that warmer temperatures (near the surface of the water body) are known to favor the attachment, growth, and multiplication of *V. cholerae* [10] (this is accounted for by assuming that, within the pond, the bacterial concentration $B_p(t)$ at time t increases according to a logistic per-biomass growth rate). The bacterial population in the pond is further increased by the influx of contaminated water from the river, at a rate $\lambda_r^* V_r^* B_r$ (where V_r^* is the constant volume of water in the river). This population is decreased by the outflow of water from the pond to the river, at a rate $\lambda_p^* B_p$, and by the natural death of the bacterium at a rate μ_B^*. Thus,

$$\dot{B}_p = \theta_p^* I + r B_p \left(1 - \frac{B_p}{k_{bp}} \right) + \lambda_r^* V_r^* B_r - \lambda_p^* B_p - \mu_B^* B_p.$$

Similarly, the bacterial population in the river is increased by shedding (at a rate θ_r^*/V_r^*) and by the influx of contaminated water from the pond, at the rate $\lambda_p^* B_p/V_r^*$. This population is decreased by the outflow of water from the river to the pond (at the rate λ_r^*) and by natural death (at the rate μ_B^*). Hence,

$$\dot{B}_r = \frac{\theta_r^*}{V_r^*} I + \lambda_p^* \frac{B_p}{V_r^*} - \lambda_r^* B_r - \mu_B^* B_r.$$

Thus, denoting with $B(t) = B_p(t) + V_r^* B_r(t)$ the total number of bacteria in the pond and the river, we obtain the following equation:

$$\dot{B} = (\theta_p^* + \theta_r^*) I + r B_p \left(1 - \frac{B_p}{k_{pb}}\right) - \mu_B^* B.$$

Since the water in the pond is generally stagnant, while the water in small rivers flow, we decided to differentiate the two water flow rates (λ_p^* for the inflow of water from the pond to the river, and λ_r^* for the inflow of water from the river to the pond and assumed that $\lambda_r^* > \lambda_p^*$). Finally, the total volume of water in the pond is increased by precipitation at a rate p and by the inflow of water from the river (at the rate λ_r^*). It is decreased by the outflow to the river (at the rate λ_p^*) and by drainage, at a rate d_r^*. This gives:

$$\dot{V}_p = p + \lambda_r^* V_r - \lambda_p^* V_p - d_r^* V_p.$$

It is assumed that there is always a minimum amount of water $V_p^{(min)} > 0$ in the pond, such that $0 < V_p^{(min)} \leq V_p(t)$ for all $t \geq 0$. This assumption guarantees water exchange between the pond and the river, in addition to sustaining *V. cholerae* transmission to the human host *via* contact with the contaminated water in the pond.

In summary, the ecology-epidemiology-hydrology model for the transmission dynamics of *V. cholerae* in a population is given by the following deterministic system of nonlinear differential equations (Figure 3 depicts a general transmission schematic of the model. The state variables and parameters of the model are described in Table 1):

$$\begin{aligned}
\dot{S} &= \Pi + \gamma^* I - \left(\beta_p^* \frac{B_p}{k_p^* V_p + B_p} + \beta_r^* \frac{B_r}{k_r + B_r}\right) S - \mu^* S, \\
\dot{I} &= \left(\beta_p^* \frac{B_p}{k_p^* V_p + B_p} + \beta_r^* \frac{B_r}{k_r + B_r}\right) S - (\gamma^* + \mu^* + \delta^*) I, \\
\dot{B}_p &= \theta_p^* I + \left[r\left(1 - \frac{B_p}{k_{bp}}\right) - \lambda_p^* - \mu_B^*\right] B_p + \lambda_r^* V_r^* B_r, \\
\dot{B}_r &= \frac{\theta_r^*}{V_r^*} I + \lambda_p^* \frac{B_p}{V_r^*} - \left(\mu_B^* + \lambda_r^*\right) B_r, \\
\dot{V}_p &= p + \lambda_r^* V_r - \left(\lambda_p^* + d_r^*\right) V_p.
\end{aligned} \tag{2.1}$$

The main assumptions in the formulation of the model (2.1) include:

1. Exponentially-distributed waiting times in each compartment of the model.
2. Recovery from cholera does not induce permanent (or partial) immunity against future *V. cholerae* infection.

3. The total volume of water in the pond ($V_p(t)$) equals or exceeds a certain minimum amount (denoted by $V_p^{(min)}$) for all time $t \geq 0$. This is the minimum amount needed to support water exchange between the pond and the river, and sustain *V. cholerae* transmission to humans from the contaminated pond. Further, the total volume of water in the river (V_r^*) is strictly positive for all time $t \geq 0$.

4. Nonlinear (Michales-Menten) incidence functions are used to account for saturation in the infection rates [10, 49].

5. No growth rate is assumed for the concentration of *V. cholerae* in the river ($B_r(t)$) [7, 8, 9, 10, 15, 41].

6. The two local water reservoirs (pond and river) are interconnected.

The model (2.1) is an extension of many of the models for cholera transmission dynamics, such as those in [7, 8, 9, 10, 15, 41, 16, 49, 51, 56], by, *inter alia*:

1. incorporating the dynamics of *V. cholerae* in an interconnected pond-river water network (i.e., we consider two different but interconnected aquatic environments for *V. cholerae* dynamics). A single water source was considered in [16, 49, 56];

2. including the inflow and outflow of water between two different aquatic environments (pond and river), not considered in ([16, 49, 56]);

3. using a nonlinear logistic function for the growth of bacteria in the pond (no bacterial growth rate is considered in [10, 15, 51, 56]; further, a linear bacterial growth function was considered in [16, 49]);

4. including an equation describing the dynamics of water volume in the pond, taking into account precipitation, drainage and water transfer to and from the river (this was not considered in [16, 49]);

5. including the possibility that humans can become infected and can spread bacteria both in the pond and in the river. Thus, we consider a dual *V. cholerae* transmission (from river and from pond) and shedding (into the river and the pond) rates. These dual transmission and shedding pathways were not taken into account in [7, 8, 9, 10, 15, 41, 16, 49, 51, 56].

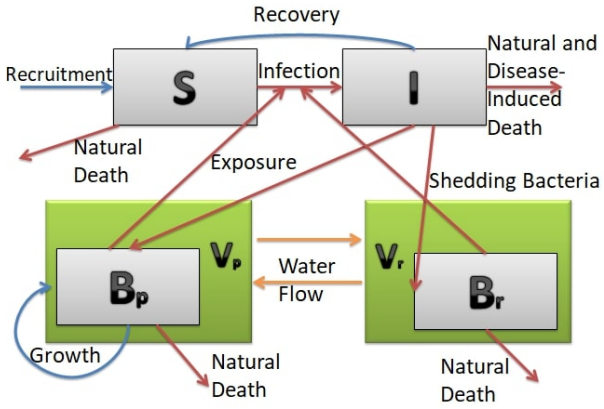

(a)

Figure 3: *V. cholerae* transmission scheme in an interconnected pond-river network

It is convenient to introduce the following change of variables and re-scaling on the model (2.1):

State Variable	Description
$S(t)$	Number of susceptible individuals at time t
$I(t)$	Number of infected individuals at time t
$B_p(t)$	*V. cholerae* number in the pond at time t
$B_r(t)$	*V. cholerae* concentration in the river at time t
$V_p(t)$	Volume of water in the pond at time t

Parameter	Description	Unit	Baseline Value	References
Π	Recruitment rate of humans (by birth or immigration)	day^{-1}	12.05	[5]
μ^*	Natural death rate of humans	day^{-1}	$9 * 10^{-5}$	[5]
γ^*	Recovery rate for human	day^{-1}	0.2	[5, 15, 51]
δ^*	Disease-induced death rate for humans	day^{-1}	$4 * 10^{-4}$	[15]
β_p^* (β_r^*)	Transmission rate in the pond (river)	day^{-1}	5 (5)	[15]
$k_p^*(k_r)$	Concentration of *V. cholerae* in the pond (river) that yields 50% chance of being infected with cholera	m^{-3}	$10^6(10^6)$	[56]
μ_B^*	Natural death rate for bacteria	day^{-1}	0.8	[5]
$\theta_p^*(\theta_r^*)$	Bacterial shedding rate in the pond (river)	day^{-1}	10^4 (10^4)	[15]
r	Reproductive rate of free-living bacteria	day^{-1}	0.3	[5, 33]
k_{bp}	Carrying-capacity of free-living bacteria in the pond	-	10^6	[33]
p	Precipitation (and river flow) rate into the pond	$m^3\text{day}^{-1}$	0.02	[51]
d_r^*	Drainage rate of the water in the pond	day^{-1}	0.02	[51]
$\lambda_p^*(\lambda_r^*)$	Rate of inflow of water from pond (river) to river (pond)	day^{-1}	0.5 (10)	Assumed
$V_p^{(min)}$	Minimum amount of water in the pond (constant) needed to support water exchange and transmission	m^3	-	-
V_r^*	Volume of water in the river (constant)	m^3	1.62×10^6	[15]

Table 1: Description of state variables and parameters of the model (2.1)

$$
\begin{aligned}
&s = \frac{S}{H}, \quad i = \frac{I}{H}, \quad b_p = \frac{B_p}{k_{bp}}, \quad b_r = \frac{B_r}{k_r}, \quad v_p = \frac{V_p}{P}, \quad t = rt^*, \\
&\beta_p = \frac{\beta_p^*}{r}, \quad \beta_r = \frac{\beta_r^*}{r}, \quad \gamma = \frac{\gamma^*}{r}, \quad \delta = \frac{\delta^*}{r}, \quad \theta_p = \frac{\theta_p^*\Pi}{\mu^* r k_{bp}}, \quad \theta_r = \frac{\theta_r^*\Pi}{r\mu^* V_r^* k_r}, \\
&\lambda_r = \frac{\lambda_r^*}{r}, \quad \lambda_p = \frac{\lambda_p^*}{r}, \quad \mu = \frac{\mu^*}{r}, \quad \mu_B = \frac{\mu_B^*}{r}, \quad d_r = \frac{d_r^*}{r}, \quad k_p = \frac{k_p^* P}{k_{bp}}, \quad V_r = \frac{V_r^* k_r}{k_{bp}},
\end{aligned}
\tag{2.2}
$$

where $P = \frac{p+\lambda_r^* V_r^*}{d_r^*+\lambda_p^*}$ and $H = \frac{\Pi}{\mu^*}$. It should be noted that the growth rate of the bacterial population in the pond (r) is now re-scaled to 1 (i.e., $r = 1$ in the normalized model (2.3)). It follows from the above re-scaling that the total human population, n, is now given by $n = s + i$. Using the change of variables and re-scaling (2.2) in the model (2.1) gives the following equivalent normalized system:

$$
\begin{cases}
\dot{s} = \mu(1-s) - \left(\beta_p \dfrac{b_p}{k_p v_p + b_p} + \beta_r \dfrac{b_r}{1+b_r}\right) s + \gamma i, \\
\dot{i} = \left(\beta_p \dfrac{b_p}{k_p v_p + b_p} + \beta_r \dfrac{b_r}{1+b_r}\right) s - (\gamma + \delta + \mu) i, \\
\dot{b}_p = \theta_p i + (1 - b_p - \mu_B - \lambda_p)\, b_p + \lambda_r V_r b_r, \\
\dot{b}_r = \theta_r i + \lambda_p \frac{b_p}{V_r} - (\mu_B + \lambda_r)\, b_r, \\
\dot{v_p} = (d_r + \lambda_p)(1 - v_p).
\end{cases}
\tag{2.3}
$$

The analysis in this study will be carried out on the normalized model (2.3). Since, like the original model

(2.1), the model (2.3) monitors the temporal dynamics of human and bacterial populations, all its state variables and parameters are non-negative.

2.1 Basic Properties of the Model

In this section, the basic qualitative properties of the normalized system (2.3) are explored. In particular, results for the existence, uniqueness, boundedness and non-negativity of its solutions are established. It is convenient to define the following sets:

$$\begin{aligned}\mathcal{D}_H &= \left\{(s,i) \in \mathbb{R}^2_+ : 0 < s + i \leq 1\right\},\\ \mathcal{D}_B &= \left\{(b_p, b_r) \in \mathbb{R}^2_+ : 0 < b_p + V_r b_r \leq b^*\right\},\\ \mathcal{D}_P &= \left\{v_p \in \mathbb{R}_+ : 0 < v_p^{(min)} \leq v_p \leq 1\right\},\end{aligned}$$

where $b^* = \dfrac{\theta_p + \theta_r V_r + \frac{1}{4}}{\mu_B} > 0$ and $v_p^{(min)} = \dfrac{V_p^{(min)}}{P} > 0$.

Let $\mathcal{D} = \mathcal{D}_H \times \mathcal{D}_B \times \mathcal{D}_P$. We claim the following result:

Theorem 2.1 *The normalized model (2.3) with initial conditions in $\mathcal{D}$ has a unique solution that exists and remains in $\mathcal{D}$ for all time t. Furthermore, the positively-invariant region $\mathcal{D}$ attracts all solutions in $\mathbb{R}^2_+ \times \mathbb{R}^2_+ \times \mathbb{R}_+$.*

Proof. Since it is clear that, for all initial solutions of the normalized model (2.3) in the region $\mathcal{D}$, the functions in the right hand-sides of the system (2.3) are locally Lipschitz in $(s, i, b_p, b_r, v_p)^T$. Hence, it follows, by the Cauchy-Lipschitz theorem, that the normalized model (2.3) admits a unique local solution. Furthermore, adding the first two equations of the system (2.3) gives (noting that $n(t) = s(t) + i(t)$)

$$\frac{dn(t)}{dt} = \mu[1 - n(t)] - \delta i(t), \tag{2.4}$$

so that,

$$\mu - (\mu + \delta)n(t) \leq \frac{dn(t)}{dt} \leq \mu[1 - n(t)].$$

Hence, it follows, by standard comparison theorem [32], that

$$0 < \frac{\mu}{\mu + \delta} \leq n(t) \leq 1, \text{ for all } t > 0 \text{ if } n(0) < 1.$$

Furthermore, it follows from Equation (2.4) that $dn(t)/dt \leq 0$ whenever $n(t) \geq 1$. Hence, the subsystem of the model (2.3) containing the equations for the dynamics of the human populations ($s(t)$ and $i(t)$) is non-negative, bounded and invariant in $\mathcal{D}_H$.

Let $b(t) = b_p(t) + V_r b_r(t)$. It follows then that the total bacterial population in the aquatic environment (i.e., bacterial populations in the pond and the river) satisfy the following equation:

$$\frac{db(t)}{dt} = (\theta_p + \theta_r V_r) i(t) + b_p(t)[1 - b_p(t)] - \mu_B b(t). \tag{2.5}$$

Since $b_p(t)[1 - b_p(t)] \leq 1/4$ for all t, and noting that $i(t) \leq 1$ in $\mathcal{D}_H$, Equation (2.5) can be written as:

$$\frac{db(t)}{dt} \leq \left(\theta_p + \theta_r V_r + \frac{1}{4}\right) - \mu_B b(t). \tag{2.6}$$

It follows, by solving the inequality (2.6), that (where $b_0 = b(0)$):

$$\begin{aligned} b(t) &\leq \frac{1}{\mu_B}\left[\theta_p + \theta_r V_r + \frac{1}{4} + \left(b_0\mu_B - \theta_p - \theta_r V_r - \frac{1}{4}\right)e^{-\mu_B t}\right], \\ &= b^*\left[1 + \frac{1}{b^*}e^{-\mu_B t}\left(b_0 - b^*\right)\right]. \end{aligned} \tag{2.7}$$

By applying a standard comparison theorem [32], the inequality (2.7) can be re-written as:

$$0 < b(t) < b^* \text{ for all } t > 0 \text{ if } 0 < b_0 \leq b^*.$$

Further, it follows from (2.6) and (2.7) that $db(t)/dt \leq 0$ whenever $b(t) \geq b^*$. Hence, the total bacterial population in the aquatic environment, $b(t)$, is bounded, non-negative and positively-invariant in $\mathcal{D}_B$.

Finally, it is clear from the last equation of (2.3) that $dv_p/dt < 0$ whenever $v_p(t) > 1$. Further, integrating this equation gives:

$$v_p(t) = 1 + (v_{\mathrm{p}_0} - 1)e^{-(d_r+\lambda_p)t},\ v_p(0) = v_{\mathrm{p}_0},$$

from which it follows that

$$\lim_{t\to+\infty} v_p(t) = 1,\ 0 < v_p(t) \leq 1 \text{ if } 0 < v_{\mathrm{p}_0} \leq 1,\ \text{and} \limsup_{t\to\infty} v_p(t) = 1.$$

Hence, the subsystem of the model (2.3) consisting of the equation for the dynamics of the water volume in the pond (v_p) is non-negative, bounded and invariant in $\mathcal{D}_P$.

In summary, it follows from the above analyses that the region $\mathcal{D}$ is positively-invariant for the normalized model (2.3), and all solutions of the normalized model are non-negative and bounded (since these results hold for the three constituent subregions, $\mathcal{D}_H$, $\mathcal{D}_B$ and $\mathcal{D}_P$). □

3 Reproduction Numbers for Various Transmission Pathways

The disease-free equilibrium of the normalized model (2.3) is given by $\mathbf{E}_0 = (s^*, i^*, b_p^*, b_r^*, v_p^*) = (1, 0, 0, 0, 1)$. Its local stability can be analysed using the next generation operator method (NGM) [22, 23, 66]. This method entails tracking the new infection terms as well as the linear transition terms in and out of infected compartments. In particular, the method involves computing two associated matrices, F (of the new infection terms) and V (of the linear transition terms), and the associated *basic reproduction number*, denoted by $\mathcal{R}_0$, is then given by $\mathcal{R}_0 = \rho(FV^{-1})$ [22, 23, 66], where ρ is the spectral radius (the dominant eigenvalue of the next generation matrix, $K = FV^{-1}$). The consequence of this approach is that the disease can be effectively controlled (or eliminated) if $\mathcal{R}_0 < 1$, and will persist in the community if $\mathcal{R}_0 > 1$. In other words, the dynamics of the disease transmission model is (often) completely determined by the reproduction number $\mathcal{R}_0$. Epidemiologically-speaking, the threshold quantity $\mathcal{R}_0$ represents the average number of new infections generated by a typical infected individual introduced into a completely susceptible population. In the context of the normalized model (2.3), the reproduction number will represent the average number of new cholera cases generated by a *V. cholerae* particle introduced the local pond-river network. It can also be a measure of the average number of *V. cholerae* particles shedded into the environment (i.e., into the pond-river network) by a typical cholera-infected human. In a recent paper, Lewis et al. [39] gave a new definition for the basic reproduction number ($\mathcal{R}_0$), which covers the definition given in [22, 23, 66], based on targeting the elements of the NGM subject to change. In particular, the Lewis et al. study establishes that $\mathcal{R}_0$ is obtained when all the elements of the NGM are targeted, whereas the type reproduction number ($\mathcal{T}$) is obtained when an entire row (or column) of the NGM is targeted.

Thus, a control strategy (e.g., vaccinating a segment of the population) that can bring (and maintain) $\mathcal{R}_0$ to a value less than unity may lead to effective control or elimination of the disease. However, for a disease with multiple population types (e.g., cholera with *V. cholerae* residing in the human host as well as in the aquatic environment (i.e., in either the local pond or river)), anti-cholera control measures can be directed to, or focussed on one, population type. This leads to a different expression for the associated reproduction number ($\mathcal{R}_0$) corresponding to each population type targeted for anti-cholera control. For instance, in the models considered in [14, 42, 63], the expressions for the associated reproduction number ($\mathcal{R}_0$) is represented as a sum of two separate terms corresponding to the host-to-host and to the environment-to-host transmission paths. This could suggest the independence of these pathways in the disease transmission cycle. Furthermore, the $\mathcal{R}_0$ for the model in [11] has a square root term that suggests a more complicated interaction between host-to-host and environment-to-host transmission pathways. It is clear from the above that, for a cholera model such as the one presented in the current study, the expression for the associated reproduction number obtained will be dependent on how the role of the environment is interpreted *vis a vis* cholera transmission dynamics (i.e., how the role of the environment is interpreted in transition between disease compartments and in transmission of secondary infectious hosts and free-living *V. cholerae* [5]). As noted by Bani-Yaghoub et al. [5], the interpretation of this role has been controversial in the literature. In particular, while numerous studies environment-host-pathogen interactions suggest that the pathogen-contaminated environment serves as a reservoir of infectious free-living pathogens for infection of various host populations (e.g., humans, other non-human animals and plants) [12, 19, 57], other studies show that the environment plays only a somewhat marginal role on the complex dynamics of infectious diseases [3, 20, 21, 40, 67] . Consequently ([5]), we hypothesize the following four scenarios where the environment acts as a (1) Transition, (2) Transition-Reservoir case I, (3) Transition-Reservoir case II and (4) Reservoir of *V. cholerae* in the environment-host-environment cholera transmission dynamics we consider in this study . In other words, the following four possible interpretations (i.e., transmission pathways) of the role the environment plays on cholera transmission dynamics will be considered for the normalized model (see also Table 2):

Scenario 1 (the environment acts as Transition): in this scenario, both the shedding of *V. cholerae* into the environment and the growth of *V. cholerae* within the environment are considered as transitions within the initial infectious state of the host population. Therefore, the the parameters of the model related to the shedding and growth rates of the bacteria are placed in the V matrix.

Scenario 2 (the environment acts as Transition-Reservoir case I): for this scenario, the growth of bacteria in the environment is regarded as vertical transmission of an infectious pathogen (*V. cholerae*) from the environment to the environment. Therefore, the parameter related to the growth rate of the bacteria in the environment (i.e., in the pond) is counted as new infection generated in the environment, and is, consequently, placed in the F matrix.

Scenario 3 (the environment acts as Transition-Reservoir case II): the environment has a double role under this scenario. In particular, while the shedding of bacteria by the host into the environment is counted as new *V. cholerae* infection, the growth of bacteria within the environment is considered as transitions within the initial infectious state of the host population (thus, the environment acts partially as reservoir and partially as transition). Consequently, the parameters related to the shedding rates are placed in the F matrix, while the parameter related to the bacteria growth in the environment (i.e., in the pond) is placed in the V matrix.

Scenario 4 (the environment acts as Reservoir): in this scenario, the environment is assumed to act as a reservoir. Hence, new infections are added into the environment both through bacteria growth (in the pond)

and bacterial shedding by infectious humans. Hence, the parameters related to both bacterial shedding and growth are placed in the F matrix.

	Cholera Transmission Rates β_p and β_r	Bacteria Shedding Rates θ_p and θ_r	Growth of Bacteria in the Pond $(r = 1)$
Scenario 1	✓		
Scenario 2	✓		✓
Scenario 3	✓	✓	
Scenario 4	✓	✓	✓

Table 2: Contributions of the various cholera transmission pathways (direct environment-host transmission and bacterial shedding) into the next generation matrix of new infection terms (F).

It is worth mentioning that Scenario 3 (where bacterial shedding rates are considered as new infections, while bacterial growth is counted as transition term) is not included in the scenarios considered in the cholera transmission model presented in [5].

It is convenient to define the following positive constants:

$$\begin{aligned} a_1 &= V_r\theta_r\lambda_r + \theta_p(\lambda_r + \mu_B), \quad & a_2 &= (\theta_p + V_r\theta_r)\lambda_p + V_r\theta_r\mu_B, \\ a_3 &= \gamma + \delta + \mu, & a_4 &= \lambda_r + \mu_B. \end{aligned} \tag{3.1}$$

The computation of the reproduction number of the normalized model (2.3), associated with each of the aforementioned scenarios, is given below.

3.1 Scenario 1 (the environment acts as Transition): pathogen shedding into, and growth within, the environment considered as transitions within the infected host population

For this setting, terms related to bacterial shedding and growth are included in the matrix V of transition terms. For this scenario, it can be shown that the associated matrices F and V are given, respectively, by

$$F_1 = \begin{pmatrix} 0 & \frac{\beta_p}{k_p} & \beta_r \\ 0 & 0 & 0 \\ 0 & 0 & 0 \end{pmatrix} \quad \text{and} \quad V_1 = \begin{pmatrix} a_3 & 0 & 0 \\ -\theta_p & \mu_B - 1 + \lambda_p & -\lambda_r V_r \\ -\theta_r & -\frac{\lambda_p}{V_r} & a_4 \end{pmatrix}, \tag{3.2}$$

so that,

$$K_1 = F_1 V_1^{-1}$$

$$= \begin{pmatrix} \frac{V_r\beta_p a_1 + k_p\beta_r(a_2 - V_r\theta_r)}{a_3 V_r k_p[a_4(\mu_B - 1) + \mu_B\lambda_p]} & \frac{k_p\beta_r\lambda_p + V_r\beta_p a_4}{V_r k_p[a_4(\mu_B - 1) + \mu_B\lambda_p]} & \frac{V_r\beta_p\lambda_r + k_p\beta_r(\lambda_p + \mu_B - 1)}{k_p[a_4(\mu_B - 1) + \mu_B\lambda_p]} \\ 0 & 0 & 0 \\ 0 & 0 & 0 \end{pmatrix}. \tag{3.3}$$

It follows that the spectral radius of NGM (K_1)is given by the quantity:

$$\mathcal{R}_0^{(1)} = \rho(K_1) = \frac{V_r\beta_p a_1 + k_p\beta_r\left[(\theta_p + V_r\theta_r)\lambda_p + V_r\theta_r(\mu_B - 1)\right]}{k_p V_r a_3[a_4(\mu_B - 1) + \mu_B\lambda_p]}, \tag{3.4}$$

that represents the average number of secondary infections through environment-to-host transmission caused by one infectious individual in its infectious lifetime, regulated respect to the bacteria growth or decay rates in the environment. It is worth noting from (3.4) that the condition $\mu_B > 1$ must be imposed to ensure that $\mathcal{R}_0^{(1)} > 0$. Hence, it is assumed, from now on, that $\mu_B - 1 \geq 0$. It should be mentioned that Bani et al. [5] assumed the strict inequality $\mu_B > 1$ (however, for our normalized model (2.3), it is possible to extend the strict inequality assumption in [5] to also include the case where $\mu_B = 1$ (there is no singularity in the normalized model when μ_B is set to 1; this is due to the interconnected nature of the pond-river network we considered in this study)).

In the context of the normalized model (2.3), the assumption $\mu_B > 1$ means that the natural death rate of bacteria (μ_B) equals the growth rate of bacteria in the pond (1; recalling that, for the normalized model (2.3), the growth rate r is re-scaled to 1). The ecological implication of this assumption is that the bacterial population in the pond ($b_p(t)$) is unable to maintain itself in the environment in the absence of human shedding (represented by θ_p). We note that this also applies to the bacterial population in the river (in fact, in the case of bacterial population in the river ($b_r(t)$), this assumption means that the $\mu_B > 0$, since, for the normalized model, the bacterial growth rate in the river is 0). Therefore, considering the entire bacterial population in the pond and in the river, the above assumption implies that the bacteria is unable to survive in the absence of infection from the host (i.e., the bacteria cannot maintain itself in the environment). It is important to underline that, with this assumption, all the entries of the NGM K_1 are non-negative and the well-posedness of $\mathcal{R}_0^{(1)}$ is ensured.

It should be mentioned that the eigenvalues of the matrix of linearization of the entire ODE system (2.3) around the disease-free equilibrium $\mathbf{E}_0$ (denoted by λ_i; $i = 1, \cdots, 5$) satisfy the quintic polynomial:

$$(\lambda + \mu)(\lambda + d_r + \lambda_p)(\lambda^3 + b_2\lambda^2 + b_1\lambda + b_0) = 0, \tag{3.5}$$

where,

$$\begin{aligned} b_2 &= a_3 + a_4 + \lambda_p + \mu_B - 1, \qquad b_0 = a_3[a_4(\mu_B - 1) + \mu_B\lambda_p]\left(1 - \mathcal{R}_0^{(1)}\right), \\ b_1 &= (a_3 + a_4)(\mu_B - 1) + a_3(a_4 + \lambda_p) + \mu_B\lambda_p - \beta_r\theta_r - \frac{\beta_p\theta_p}{k_p}. \end{aligned} \tag{3.6}$$

It follows from the first two terms of (3.5) that the eigenvalues $\lambda_1 = -\mu < 0$ and $\lambda_2 = -(d_r + \lambda_p) < 0$. Further, it follows from (3.6) that the coefficients b_2 and b_0 of the cubic in (3.5) are automatically positive for $\mu_B - 1 \geq 0$ and $\mathcal{R}_0^{(1)} < 1$. It can also be shown, with algebraic manipulations, that the coefficient $b_1 > 0$ whenever $\mathcal{R}_0^{(1)} < 1$. It is convenient to assume that $\lambda_p \geq 1$. It follows then that the associated Routh-Hurwitz condition $b_2 b_1 - b_0 > 0$ holds if and only if $\mathcal{R}_0^{(1)} < 1$ (see Appendix A1). Hence, the

roots of the cubic in (3.5) have negative real part whenever $\mathcal{R}_0^{(1)} < 1$. Thus, the disease-free equilibrium ($\mathbf{E}_0$) of the normalized model (2.3) is locally-asymptotically stable whenever $\mathcal{R}_0^{(1)} < 1$. In other words, the application of the method of standard linearization (around the disease-free equilibrium of the normalized model) corresponds to Scenario 1 of this study. It is noteworthy that the matrix F_1 (and also K_1) is rank 1 (corresponding to the associated single transmission pathway).

3.2 Scenario 2 (the environment acts as Transition-Reservoir case I): growth of bacteria regarded as vertical transmission of *V. cholerae* in the environment

Here, the bacterial growth term is considered as a new infection of the environment. That is, the bacteria growth rate is placed in the F matrix. For this setting,

$$F_2 = \begin{pmatrix} 0 & \frac{\beta_p}{k_p} & \beta_r \\ 0 & 1 & 0 \\ 0 & 0 & 0 \end{pmatrix} \text{ and } \quad V_2 = \begin{pmatrix} a_3 & 0 & 0 \\ -\theta_p & \mu_B + \lambda_p & -\lambda_r V_r \\ -\theta_r & -\frac{\lambda_p}{V_r} & a_4 \end{pmatrix}. \tag{3.7}$$

Thus,

$$K_2 = F_2 V_2^{-1} = \begin{pmatrix} \frac{V_r\beta_p(V_r\theta_r\lambda_r a_4\theta_p)+k_p\beta_r(\theta_p\lambda_p+V_r\theta_r(\lambda_p+\mu_B))}{k_pV_r\mu_B a_3(a_4+\lambda_p)} & \frac{V_r\beta_p a_4+k_p\beta_r\lambda_p}{k_pV_r\mu_B(a_4+\lambda_p)} & \frac{V_r\beta_p\lambda_r+k_p\beta_r(\lambda_p+\mu_B)}{k_p\mu_B(a_4+\lambda_p)} \\ \frac{V_r\theta_r\lambda_r+\theta_p a_4}{a_3\mu_B(a_4+\lambda_p)} & \frac{a_4}{\mu_B(a_4+\lambda_p)} & \frac{V_r\lambda_r}{\mu_B(a_4+\lambda_p)} \\ 0 & 0 & 0 \end{pmatrix}. \tag{3.8}$$

Therefore,

$$\mathcal{R}_0^{(2)} = \rho(K_2) = \frac{g_1 + \sqrt{g_1^2 + 4g_2}}{2}, \tag{3.9}$$

where,

$$g_1 = \frac{V_r\beta_p a_1 + k_p\beta_r a_2 + V_r k_p a_3 a_4}{k_p V_r \mu_B a_3(a_4 + \lambda_p)}, \quad g_2 = \frac{\beta_r\theta_r}{\mu_B a_3(a_4 + \lambda_p)}. \tag{3.10}$$

The expression for $\mathcal{R}_0^{(2)}$, given by (3.9), suggests a more complicated interaction of the environment-to-host and host-to-host pathways (in comparison to $\mathcal{R}_0^{(1)}$ for Scenario 1). Further, it is worth noting that the matrix F_2 (and also K_2) is rank 2 (corresponding to the two transmission pathways associated with Scenario 2).

3.3 Scenario 3 (the environment acts as Transition-Reservoir case II): shedding of bacteria considered as new infections but bacterial growth is a transition term

In this scenario, bacterial shedding rates are placed in the F matrix, while the bacterial growth rate is placed in the V matrix. Here,

$$F_3 = \begin{pmatrix} 0 & \frac{\beta_p}{k_p} & \beta_r \\ \theta_p & 0 & 0 \\ \theta_r & 0 & 0 \end{pmatrix} \text{ and } \quad V_3 = \begin{pmatrix} a_3 & 0 & 0 \\ 0 & \mu_B - 1 + \lambda_p & -\lambda_r V_r \\ 0 & -\frac{\lambda_p}{V_r} & a_4 \end{pmatrix}, \tag{3.11}$$

so that,

$$K_3 = F_3 V_3^{-1} = \begin{pmatrix} 0 & \frac{V_r\beta_p a_4 + k_p\beta_r\lambda_p}{k_p V_r[a_4(\mu_B-1)+\lambda_p\mu_B]} & \frac{V_r\beta_p\lambda_r + k_p\beta_r(\lambda_p+\mu_B-1)}{k_p[a_4(\mu_B-1)+\lambda_p\mu_B]} \\ \frac{\theta_p}{a_3} & 0 & 0 \\ \frac{\theta_r}{a_3} & 0 & 0 \end{pmatrix}, \tag{3.12}$$

and,

$$\mathcal{R}_0^{(3)} = \rho(K_3) = \sqrt{\frac{V_r\beta_p a_1 + k_p\beta_r\left[(\theta_p + V_r\theta_r)\lambda_p + V_r\theta_r(\mu_B-1)\right]}{k_p V_r a_3[a_4(\mu_B-1)+\mu_B\lambda_p]}}. \tag{3.13}$$

It should be noted that the quantity $\mathcal{R}_0^{(3)} > 0$ (whenever $\mu_B - 1 \geq 0$). Furthermore, it is clear that $\mathcal{R}_0^{(1)} = \left(\mathcal{R}_0^{(3)}\right)^2$. For this scenario, the associated matrix of new infections (F_3) is rank 2 (corresponding to the two associated transmission pathways; the matrix K_3 is also rank 2).

3.4 Scenario 4 (the environment acts as Reservoir): the environment is assumed to act as a reservoir

In this case, both bacterial growth and shedding are considered as new infections of the environment. Hence, both the shedding and growth rates are placed in the F matrix. For this scenario,

$$F_4 = \begin{pmatrix} 0 & \frac{\beta_p}{k_p} & \beta_r \\ \theta_p & 1 & 0 \\ \theta_r & 0 & 0 \end{pmatrix} \text{ and } \quad V_4 = \begin{pmatrix} a_3 & 0 & 0 \\ 0 & \mu_B + \lambda_p & -\lambda_r V_r \\ 0 & -\frac{\lambda_p}{V_r} & a_4 \end{pmatrix}, \tag{3.14}$$

so that,

$$K_4 = F_4 V_4^{-1} = \begin{pmatrix} 0 & \frac{V_r\beta_p a_4 + k_p\beta_r\lambda_p}{k_p V_r\mu_B(a_4+\lambda_p)} & \frac{V_r\beta_p\lambda_r + k_p\beta_r(\lambda_p+\mu_B)}{k_p\mu_B(a_4+\lambda_p)} \\ \frac{\theta_p}{a_3} & \frac{a_4}{\mu_B(a_4+\lambda_p)} & \frac{V_r\lambda_r}{\mu_B(a_4+\lambda_p)} \\ \frac{\theta_r}{a_3} & 0 & 0 \end{pmatrix}. \tag{3.15}$$

Hence, it follows that $\mathcal{R}_0^{(4)} = \rho(K_4)$ is the spectral radius of the following associated characteristic polynomial (of K_4):

$$p(\lambda) = \lambda^3 + d_2\lambda^2 + d_1\lambda + d_0, \tag{3.16}$$

where,

$$d_2 = -\frac{a_4}{\mu_B(a_4+\lambda_p)}, \quad d_1 = -\frac{V_r\beta_p(V_r\theta_r\lambda_r+\theta_p a_4)+k_p\beta_r[\theta_p\lambda_p+V_r\theta_r(\lambda_p+\mu_B)]}{k_p a_3 V_r\mu_B(a_4+\lambda_p)},$$
$$d_0 = \frac{\beta_r\theta_r}{a_3\mu_B(a_4+\lambda_p)}. \tag{3.17}$$

The discriminant of the cubic (3.16) is given by [65]:

$$\Delta_p = d_2^2d_1^2 + 18d_1d_2d_0 - 4d_1^3 - 4d_0d_2^3 - 27d_0^2,$$

and it can be shown, after some algebraic manipulations, that $\Delta_p > 0$ (see Appendix A). Thus, all three roots of the cubic (3.16) are real. Moreover, since the coefficients $d_2 < 0$, $d_1 < 0$ and $d_0 > 0$, it follows, by the Descartes's Rule of Signs ([38]), that $p(\lambda)$ has two positive and one negative real roots. Therefore, its largest root (i.e., $\mathcal{R}_0^{(4)}$) is real and positive, and is given by (obtained from solving the cubic (3.16) [65]):

$$\mathcal{R}_0^{(4)} = \sqrt[3]{-\frac{q_1}{2}+\sqrt{\frac{q_1^2}{4}+\frac{q_2^3}{27}}} + \sqrt[3]{-\frac{q_1}{2}-\sqrt{\frac{q_1^2}{4}+\frac{q_2^3}{27}}}, \tag{3.18}$$

where,

$$q_1 = -\frac{m_1+m_2}{27k_pV_r\mu_B^3a_3(a_4+\lambda_p)^3},$$
$$q_2 = -\frac{3V_r\beta_p\mu_B(a_4+\lambda_p)a_1 + k_p(V_ra_3a_4^2+3\beta_r\mu_B(a_4+\lambda_p)a_2)}{3k_pV_r\mu_B^2a_3(a_4+\lambda_p)^2}, \tag{3.19}$$

with,

$$m_1 = 9V_r\beta_p\mu_Ba_4(a_4+\lambda_p)a_1,$$

$$m_2 = k_p(2V_ra_3a_4^3 + 9\beta_r\mu_B(a_4+\lambda_p)(\theta_p\lambda_pa_4 + V_r\theta_r(\lambda_r(\lambda_p-2\mu_B)-2\mu_B(\lambda_p+\mu_B)))).$$

The matrix F_4 (and also K_4) is rank 3 (corresponding to the associated three transmission pathways).

In summary, the analyses in this section reveal that, by considering multiple transmission pathways, multiple reproduction numbers were obtained for the normalized model (2.3). The fact that these reproduction numbers are not unique may lead to the possible underestimation or overestimation of the control efforts needed to effectively control or eliminate the disease. To address this problem (of lack of uniqueness of the reproduction threshold associated with disease transmission dynamics), Roberts and Heesterbeek [52] and Heesterbeek and Roberts [30] introduced the notion of *type reproduction number*, denoted by $\mathcal{T}$. This allows for the determination of a single threshold quantity that is valid for each of the four scenarios described above (and listed in Table 2).

The four basic reproduction numbers ($\mathcal{R}_0^{(i)}$; $i = 1, \cdots, 4$) computed above are compared as follows. In particular, a plot of each of the reproduction as a function of bacterial shedding rate in the river (θ_r) and as a function of cholera transmission rate in the river (β_r) are depicted in Figure 4 (left and right panels, respectively). This figure shows that, with the assumption $\mu_B - 1 \geq 0$, all four basic reproduction numbers agree on the threshold value 1(i.e., unity). That is,

$$\mathcal{R}_0^{(1)} = 1 \Leftrightarrow \mathcal{R}_0^{(2)} = 1 \Leftrightarrow \mathcal{R}_0^{(3)} = 1 \Leftrightarrow \mathcal{R}_0^{(4)} = 1. \tag{3.20}$$

Further, for a fixed set of parameter values, numerical simulations (Figure 4) suggest that the four reproduction numbers are all greater, equal or less than unity. It was further observed that when any of the basic reproduction numbers exceeds unity, the following ordering always holds:

$$\mathcal{R}_0^{(1)} > \mathcal{R}_0^{(2)} > \mathcal{R}_0^{(3)} > \mathcal{R}_0^{(4)} > 1.$$

The order is reversed if any of the basic reproduction numbers is less than unity (that is, $\mathcal{R}_0^{(1)} < \mathcal{R}_0^{(2)} < \mathcal{R}_0^{(3)} < \mathcal{R}_0^{(4)} < 1$). It should be mentioned that a partial (inequality) ordering of the reproduction numbers ($\mathcal{R}_0^{(i)},\ i = 1, ..., 4$) can be obtained analytically by applying Theorem 7 in [39] (see Appendix B for details).

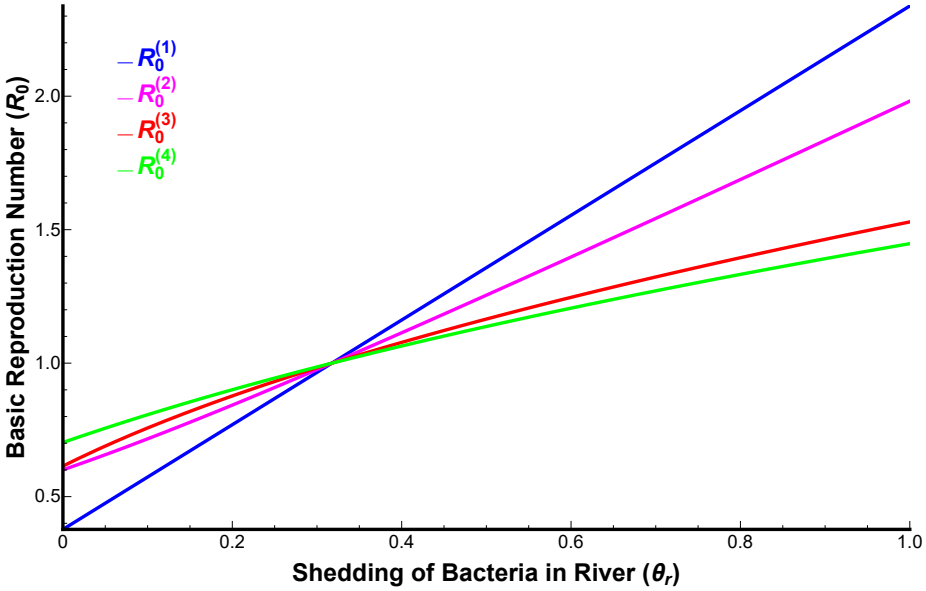

(a)

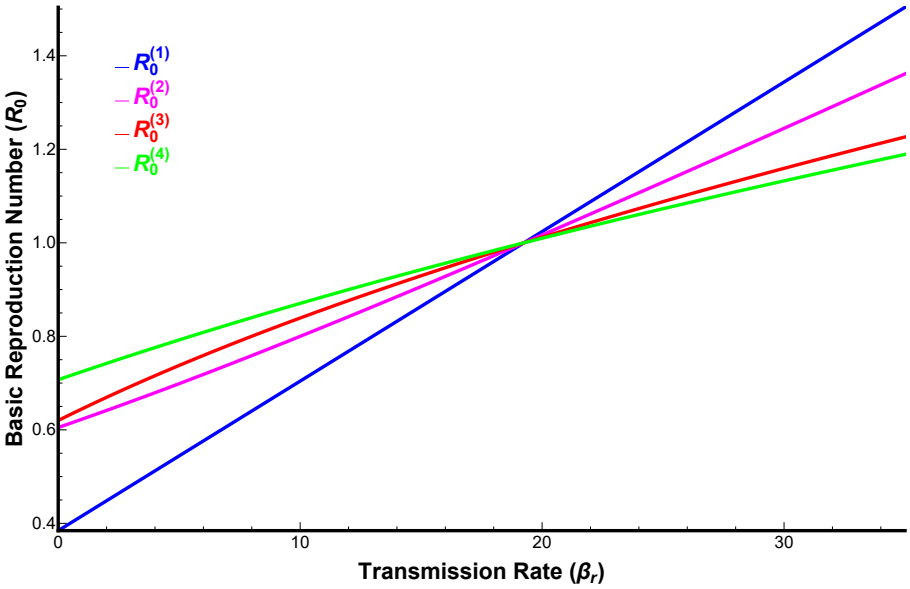

(b)

Figure 4: The plots represent the behaviours of the different expression of $\mathcal{R}_0$ derived: $\mathcal{R}_0^{(1)}$ is the blue line, $\mathcal{R}_0^{(2)}$ magenta line, $\mathcal{R}_0^{(3)}$ the red line and $\mathcal{R}_0^{(4)}$ the green line. The parameter values used are listed in Table 1 with $\theta_p = 10^3$. $\mathcal{R}_0$ is a function of the parameter θ_r in graph (a) and of β_r in graph (b).

4 Type Reproduction Number

First of all, it should be noted that the entry k_{ij} of the NGM K is defined as the expected number of new cases that a infected individual of type j causes among the susceptible individuals of type i, in a fully susceptible population. To prevent or mitigate an outbreak of a disease, preventive intervention measures (such as vaccination, quarantine, isolation, public health education etc.) are generally implemented, depending on the type of the disease and availability of control resources. If these interventions are implemented to all the sub-populations involved in the disease transmission cycle, regardless of their infection status, then the quantity $\mathcal{R}_0$ also provides a measure of the minimum coverage level of the adopted control measures needed to eliminate the disease [2, 22]. Otherwise, if a control strategy is aimed only at particular population type, such as the use of chemical insecticides to control bacterial population in the aquatic environment or vaccinating the human hosts, the so-called type reproduction number (denoted by $\mathcal{T}_s$, where s is the population type) takes on the role of $\mathcal{R}_0$ (hence, it also has a direct relationship with the minimum coverage level of the control strategy or strategies implemented) [30, 52]. In other words, the threshold quantity $\mathcal{R}_0$ (or, in this case, equivalently, $\mathcal{T}_s$) provides a measure of the effort (or coverage level) required to achieve population-wide elimination of the disease when the adopted control interventions are aimed at a particular type of population.

In the context of the normalized model (2.3), let humans represent population of type 1. Further, let the bacterial population in the pond and in the river represent bacterial populations of type 2 and 3, respectively. Let k be the number of disease transmission scenarios considered (i.e., $k = 1, \cdots, 4$, as discussed in Section 3) . It then follows that, in most cases, a strategy that reduces the susceptibility to infection of humans (type 1), for example, influences all the entries of the NGM that represents potentially infectious contacts between the bacterium and a susceptible of type 1 (i.e., a susceptible human). Mathematically-speaking, this strategy affects the entries of the first row of the NGM (K). Similarly, a strategy aimed at reducing the infectiousness of infected humans (type 1) affects the entries of the first column of the NGM K [5, 30, 39]. It is worth recalling the following definition.

Definition 4.1 *[30, 52] The type reproduction number ($\mathcal{T}_s$) associated with the population type s is defined by*

$$\mathcal{T}_s^{(j)} = \boldsymbol{e}_s^T K_j [I - (I - P_s)K_j]^{-1} \boldsymbol{e}_s, \ j = 1, \cdots, k \tag{4.1}$$

where K_j is a given NGM of order n related to Scenario j, I is the $n \times n$ identity matrix, $\boldsymbol{e}_s$ is an n-dimensional column vector with all entries zero except that the s entry is equal to 1, and P_s is a projection matrix with the (s, s) entry equal to 1 and all other entries equal to zero.

Using the notation in [5], let $K_i = F_i V_i^{-1}$ $(i = 1, ..., k)$ be the NGMs obtained from different epidemiological scenarios. Further, assume (without loss of generality) that [5]

$$V_j = V_i + U_m \text{ and } F_j = F_i + U_m, \ \{i, j\} \in \{1, ..., k\}, \text{ with } i \neq j, \tag{4.2}$$

where U_m is a matrix with m non-zero rows (say, rows $l_1, ..., l_m$, which correspond to the m disease compartments above) and $n - m$ zero rows. Furthermore, V_i and F_i are transition and transmission matrices corresponding to Scenario i, respectively, while V_j and F_j are the transition and transmission matrices corresponding to Scenario j, respectively (with $i \neq j$). It is convenient to recall the following result (proved in [5]):

Theorem 4.1 *[5] Let $\mathcal{T}_s^i$ and $\mathcal{T}_s^j$ be the type reproduction numbers associated with population type s defined by (4.1) and, respectively, derived from the NGMs K_i and K_j, with $\{i, j\} \in \{1, ..., k\}$, with $i \neq j$. If $s \neq l_w$, with $w = 1, ..., m$ and both $\mathcal{T}_s^i$ and $\mathcal{T}_s^j$ are well defined, then $\mathcal{T}_s^i = \mathcal{T}_s^j$.*

Theorem 4.1 will be used to determine whether or not the type reproduction number computed for each of the three populations types will be unique for all four scenarios discussed in Section 3 (by showing whether or not the hypotheses of the above theorem are satisfied for each case).

The normalized model (2.3) has $n = 3$ disease compartments (i.e., $i(t)$, $b_p(t)$ and $b_r(t)$) and, the value of the parameter m (for the interactions within and between the disease compartments $b_p(t)$ and $b_r(t)$) depends on the scenarios being compared. For example, if we consider Scenarios 1 and 2, only the role of the compartment $b_p(t)$ is interpreted differently (since, in Scenario 1, the bacteria growth parameter ($r = 1$) is placed in the V_1 matrix, while in Scenario 2 it is placed in the F_2 matrix). Hence, in this case, $m = 1$. If we, instead, compare Scenario 1 with Scenario 3 or Scenario 4, then $m = 2$ (since, in this case, both $b_p(t)$ and $b_r(t)$ are epidemiologically interpreted differently; for example, in Scenario 1 the parameters for the shedding rate of bacteria, represented by θ_p and θ_r, are placed in the V_1 matrix, while in Scenario 3 they are placed in the F_3 matrix).

4.1 Targeting population of type 1 (humans)

In Section 3, we showed four different scenarios, leading to different NGM (K_i, with $i = 1, 2, 3, 4$). For the normalized model (2.3), the total number of *V. cholerae* transmission scenario considered is four (i.e., $k = 4$). Here, consider population of type $s = 1$ (that is, we consider the compartment $i(t)$). Therefore, in order to apply Definition (4.1) for the computation of the associated type reproduction numbers ($\mathcal{T}_1^{(j)}; j = 1, \cdots, 4$), the associated vector $\mathbf{e}_1$ and projection matrix P_1 are introduced as follows:

$$\mathbf{e}_1 = \begin{pmatrix} 1 \\ 0 \\ 0 \end{pmatrix}, \quad P_1 = \begin{pmatrix} 1 & 0 & 0 \\ 0 & 0 & 0 \\ 0 & 0 & 0 \end{pmatrix}. \tag{4.3}$$

Considering Scenario 1 (i.e., $j = 1$) and substituting $j = 1$ (and using K_1, $\mathbf{e}_1$ and P_1) into (4.1), one gives the the following associated type reproduction number related to (targeting) the infected human population $i(t)$ (i.e., $s = 1$):

$$\begin{aligned} \mathcal{T}_1^{(1)} &= \mathbf{e}_1^T K_1 [I - (I - P_1)K_1]^{-1} \mathbf{e}_1, \\ &= \frac{V_r \beta_p a_1 + k_p \beta_r \left[(\theta_p + V_r \theta_r)\lambda_p + V_r \theta_r (\mu_B - 1)\right]}{k_p V_r a_3 [a_4(\mu_B - 1) + \mu_B \lambda_p]}, \end{aligned} \tag{4.4}$$

where K_1 is the NGM of Scenario 1 given in (3.3). Now it is proved that the same expression for $\mathcal{T}_1^{(1)}$ is obtained in the other three transmission scenarios. First of all, it can be shown that Assumption (4.2) holds for the normalized model (2.3). Indeed, if $i = 1$ and $j = 2$ (i.e., if we compare Scenario 1 and Scenario 2), then it follows from (4.2) that (note that $m = 1$ in this case):

$$V_2 = V_1 + U_1, \text{ and } F_2 = F_1 + U_1,$$

where,

$$U_1 = \begin{pmatrix} 0 & 0 & 0 \\ 0 & 1 & 0 \\ 0 & 0 & 0 \end{pmatrix}.$$

In this case, we have $l_1 = 2$ (the second row of U_m (or, equivalently, U_1) corresponds to the compartment b_p, that is interpreted differently).

Moreover, if $i = 1$ and $j = 3$ (i.e., if Scenario 1 and Scenario 3 are compared), Equation (4.2) gives (note that $m = 2$ in this case):

$$V_3 = V_1 + U_2, \text{ and } F_3 = F_1 + U_2,$$

where,

$$U_2 = \begin{pmatrix} 0 & 0 & 0 \\ \theta_p & 0 & 0 \\ \theta_r & 0 & 0 \end{pmatrix}.$$

In this case, we have $l_1 = 2$ and $l_2 = 3$ (the second and third rows of U_m (i.e., U_2 in this case) correspond to the compartments b_p and b_r, that are interpreted differently). Finally, if $i = 1$ and $j = 4$ (i.e., we comparing Scenario 1 and Scenario 4), it then follows from (4.2) that (noting that $m = 2$ in this case):

$$V_4 = V_1 + U_2, \text{ and } F_4 = F_1 + U_2,$$

where,

$$U_2 = \begin{pmatrix} 0 & 0 & 0 \\ \theta_p & 1 & 0 \\ \theta_r & 0 & 0 \end{pmatrix}.$$

In this case, $l_1 = 2$ and $l_2 = 3$ (the second and third rows of U_m correspond to the compartments b_p and b_r, that are interpreted differently). It should be mentioned that these can, of course, also be achieved by comparing all other scenario permutations (i.e., comparing Scenario 2 with Scenario 3, or Scenario 2 with Scenario 4 or Scenario 3 with Scenario 4).

Second, let $\mathcal{T}_1^i$ ($i = 1, 2, 3, 4$) be the type reproduction numbers associated with population type $s = 1$ defined by (4.1) and, respectively, derived from the NGMs K_i ($i = 1, 2, 3, 4$). It has just been pointed out that there can be at most two compartments that are interpreted differently in the scenarios considered, which are $b_p(t)$ (which corresponds to $s = 2$) and $b_r(t)$ (which corresponds to $s = 3$). So the compartment that is targeted here, $i(t)$ (which corresponds to $s = 1$), is interpreted the same way in all scenarios. It is easy to see that the hypotheses of the Theorem 4.1 are verified. Since in this case with humans as the population type considered (i.e., $s = 1$), and for all the aforementioned scenarios we compared $s = 1$ always differs from l_1 and l_2 (with $l_1 = 2$ and $l_2 = 3$), it follows from Theorem 4.1 that the associated type reproduction number ($\mathcal{T}_1$) is unique. Indeed, $s = 1$ is different from l_w ($w = 1, 2$), when Scenario 1 is compared with the other three scenarios. Hence, regardless of how the associated human-bacteria interactions are interpreted, the type reproduction number related to the infected human host population ($i(t)$) is unique. That is, the following result holds (by Theorem 4.1 [5]):

$$\mathcal{T}_1 = \mathcal{T}_1^{(j)} = \mathcal{R}_0^{(1)} = \left(\mathcal{R}_{\mathbf{0}}^{(\mathbf{3})}\right)^{\mathbf{2}}, \quad \text{for} \quad j = 1, \cdots, 4. \tag{4.5}$$

Noting that $\mu_B - 1 \geq 0$, it follows from the expression of $\mathcal{R}_0^{(1)}$ given in Section 3 that $\mathcal{T}_1^j$ is well defined for $j = 1, \cdots, 4$ (corresponding, respectively, to Scenarios 1, 2, 3 and 4 in Section 3). The result below follows from Theorem 2 of [66].

Theorem 4.2 *The disease-free equilibrium point, $\boldsymbol{E}_0$ of the normalized model (2.3), is locally-asymptotically stable if $\mathcal{T}_1 < 1$ (or, equivalently, $\mathcal{R}_0^{(1)} < 1$), and unstable if $\mathcal{T}_1 > 1$ (or, equivalently, $\mathcal{R}_0^{(1)} > 1$), where $\mathcal{T}_1$ is the associated type reproduction number defined in (4.5).*

The epidemiological implication of Theorem 4.2 is that a small influx of infected individuals (i.e., in the basin of attraction of the disease-free equilibrium $\mathbf{E}_0$) will not cause a major outbreak in the community. In

other words, cholera can be eliminated from the community if the initial number of individuals is not large enough. To ensure that disease elimination is not dependent on the initial number of infected individuals, a global asymptotic stability result must be established for the disease-free equilibrium $\mathbf{E}_0$. This is done below for a special case where the volume of water in the pond is maximum (i.e., $v_p(t) = 1$). Targeting the human population could correspond to the implementation of a strategy, such as a routine vaccination program or treatment of confirmed cases, that reduces β_p and β_r.

Theorem 4.3 *Consider the special case of the normalized model (2.3) with $v_p(t) = 1$ for all t. The disease-free equilibrium, $\boldsymbol{E}_0$, of the model is globally-asymptotically stable in $\mathcal{D}$ if $\mathcal{T}_1 < 1$ (or, equivalently, if $\mathcal{R}_0^{(1)} = \left(\mathcal{R}_0^{(3)}\right)^2 < 1$), and unstable if $\mathcal{T}_1 > 1$ (or, equivalently, if $\mathcal{R}_0^{(1)} = \left(\mathcal{R}_0^{(3)}\right)^2 > 1$).*

The proof of Theorem 4.3, based on using a Lyapunov function theory and LaSalle's Invariance Principle [37], is given in Appendix C. It is worth mentioning that the results of Theorems 4.2 and 4.3 also hold (but only with respect to the reproduction number, $\mathcal{R}_0^{(j)}$; $j = 1, \cdots, 4$) when the other population types (i.e., $s = 2$ or $s = 3$) are targeted (Bani et al. [5] also showed that the disease-free equilibrium of their cholera model is globally-asymptotically stable whenever any of the constituent reproduction number of the model is less than unity).

The epidemiological implication of Theorem 4.3 is that bringing (and maintaining) the Type reproduction number ($\mathcal{T}_1$ or, equivalently, $\mathcal{R}_0^{(1)}$ or $\mathcal{R}_0^{(3)}$) to a value less than unity is necessary and sufficient for the elimination of cholera from the population. Further, following Bani et al. [5], this result can be expressed in terms of the *herd immunity threshold*. In particular, a control strategy that targets the population type 1 (i.e., bacteria in the human host) can lead to the effective control or elimination of the disease if the control is administered to at least the proportion

$$p_1^{(j)} = 1 - \frac{1}{\mathcal{R}_0^{(1)}} = 1 - \frac{1}{\mathcal{T}_1} \text{ (with } j = 1, 2, 3, 4),$$

of the human host population. Using a simple model for the 2006 cholera epidemic in Angola (which accounts for direct and indirect cholera transmission with a single *V. cholerae* compartment), Eisenberg et al. [24] estimate $\mathcal{R}_0$ in the range $\mathcal{R}_0 \in [1.32, 5.9]$. Thus, based on this data (and estimates), our study shows that, for the best-case scenario (with $\mathcal{R}_0 = 1.32$), the control need to be implemented to at least 24.2% of the human host population. For the worst-case scenario (with $\mathcal{R}_0 = 5.9$), the control need to be administered to at least 83% of the human host population. It should be emphasized that, for the purpose of disease control, the herd immunity threshold can also be computed in terms of the basic reproduction number, and without targeting any specific disease or environmental compartments, using the relation [34] (where the subscript representing the population type considered is now omitted):

$$p^{(i)} = 1 - \frac{1}{\mathcal{R}_0^{(i)}}, \; i = 1, \cdots, 4.$$

The drawback associated with using $\mathcal{R}_0^{(i)}$ to compute the herd immunity threshold is the fact that there will now be a different threshold for each individual scenario (due to this reason, we exclusively use the type reproduction number to compute the herd immunity threshold for each targeted population type).

It is worth emphasizing that the above theoretical results hold only when $\mu_B \geq 1$. Otherwise (i.e., if $\mu_B < 1$), the environment becomes a reservoir of the pathogen and control measures acting on the host human population will not be sufficient to eradicate the infection. Moreover, if $\mu_B < 1$, then additional conditions need to be imposed on the model parameters to ensure the positivity of the associated threshold quantities, $\mathcal{R}_0^{(i)}$ (with $i = 1, 2, 3, 4$). Similar conditions need to be imposed on $\mathcal{T}_1$ as well. The results of Theorems 4.2 and 4.3 are numerically illustrated by simulating the normalized model (2.3) using parameter

values such that $\mathcal{R}_0^{(i)} < 1$ ($i = 1, \cdots, 4$) (equivalently, $\mathcal{T}_1 < 1$). The results obtained, depicted in Figure 5, show convergence of initial conditions to the DFE $\mathbf{E}_0$ in all the four transmission scenarios considered.

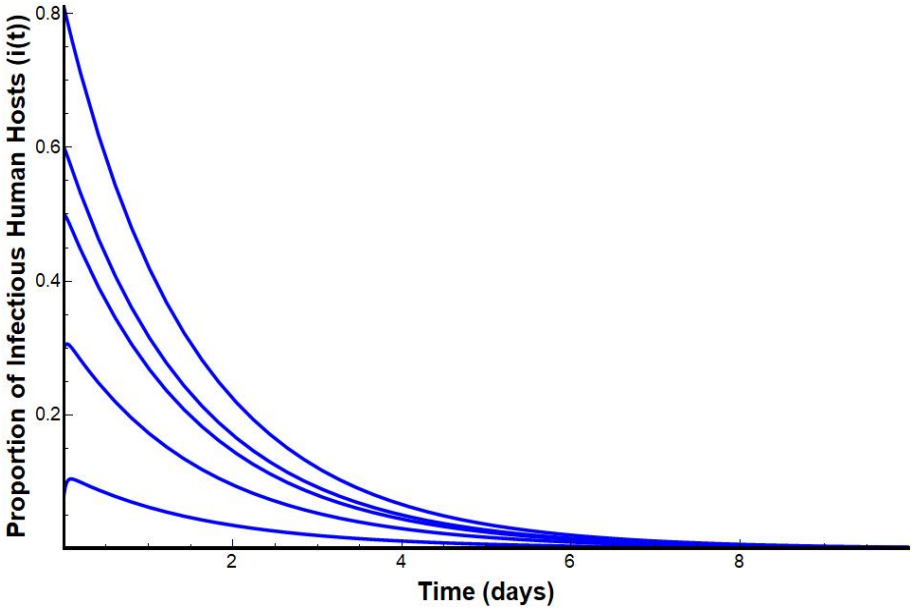

Figure 5: Numerical simulations of the normalized model (2.3) showing convergence to 0 of multiple initial conditions. Parameter values used are as given in Table 1 with $\beta_p^* = \beta_r^* = 2$ and $\theta_p^* = \theta_r^* = 10^3$ (so that, $\mathcal{R}_0^{(1)} = \mathcal{T}_1 = 0.37$, $\mathcal{R}_0^{(2)} = 0.57$, $\mathcal{R}_0^{(3)} = 0.61$ and $\mathcal{R}_0^{(4)} = 0.68$).

4.2 Targeting population of type 2 (bacteria in the pond)

Suppose, now, that an anti-cholera control measure (e.g., the use of chemical insecticides) is implemented only on population of type 2 (i.e., bacteria in the pond). In this case, it follows from Definition (4.1) that the vector $\mathbf{e}_2$ and projection matrix P_2 are given, respectively, by:

$$\mathbf{e}_2 = \begin{pmatrix} 0 \\ 1 \\ 0 \end{pmatrix} \text{ and } \quad P_2 = \begin{pmatrix} 0 & 0 & 0 \\ 0 & 1 & 0 \\ 0 & 0 & 0 \end{pmatrix}. \tag{4.6}$$

Substituting $j = 1$ (and using the NGM K_1, $\mathbf{e}_2$ and P_2) into (4.1) gives the following type reproduction number for Scenario 1 (for $s = 2$):

$$\mathcal{T}_2^{(1)} = \mathbf{e}_2^T K_1 [I - (I - P_2)K_1]^{-1} \mathbf{e}_2 = 0. \tag{4.7}$$

Indeed, in Scenario 1, the growth rate of bacteria in the pond ($r = 1$) and the shedding rates (θ_p and θ_r) are placed in the matrix V, as transitions within the populations. In fact, in Scenario 1, only the human host (and not any of the other two population types) contribute to the matrix F of new infection terms. Thus, targeting the type 2 population (i.e., the pond) has no effect in hindering the generation of new infected individuals (i.e., targeting $b_p(t)$ does not contribute to the matrix F of new infections).

For Scenario 2, setting $j = 2$ (and using the NGM K_2, $\mathbf{e}_2$ and P_2) into (4.1) gives the following type reproduction number for Scenario 2 (for $s = 2$):

$$\begin{aligned}\mathcal{T}_2^{(2)} &= \mathbf{e}_2^T K_2[I-(I-P_2)K_2]^{-1}\mathbf{e}_2,\\ &= \frac{k_p V_r(\beta_r\theta_r - a_3a_4)}{V_r\beta_p a_1 + k_p\beta_r a_2 - V_r\mu_B k_p a_3(a_4+\lambda_p)},\end{aligned} \tag{4.8}$$

provided $\mathcal{T}_2^{(2)} > 0$. Similarly, setting $j = 3$ (and using the NGM K_3, $\mathbf{e}_2$ and P_2) into (4.1) gives the following type reproduction number for Scenario 3 (for $s = 2$):

$$\begin{aligned}\mathcal{T}_2^{(3)} &= \mathbf{e}_2^T K_3[I-(I-P_2)K_3]^{-1}\mathbf{e}_2,\\ &= \frac{\theta_p[V_r\beta_p a_4 + k_p\beta_r\lambda_p]}{-V_r[\beta_p V_r\lambda_r\theta_r + k_p\beta_r\theta_r(\lambda_p+\mu_B-1) - k_p a_3(a_4(\mu_B-1)+\lambda_p\mu_B)]},\end{aligned} \tag{4.9}$$

provided $\mathcal{T}_2^{(3)} > 0$. Finally, setting $j = 4$ (and using the NGM K_4, $\mathbf{e}_2$ and P_2)) into (4.1) gives the following type reproduction number for Scenario 4 (for $s = 2$):

$$\begin{aligned}\mathcal{T}_2^{(4)} &= \mathbf{e}_2^T K_4[I-(I-P_2)K_4]^{-1}\mathbf{e}_2,\\ &= \frac{-V_r\beta_p\theta_p a_4 - k_p\beta_r\lambda_p\theta_p + k_p V_r(\beta_r\theta_r - a_3a_4)}{V_r[\beta_p V_r\lambda_r\theta_r + k_p\beta_r\theta_r(\lambda_p+\mu_B) - k_p\mu_B a_3(a_4+\lambda_p)]},\end{aligned} \tag{4.10}$$

provided $\mathcal{T}_2^{(4)} > 0$. Since the interactions between the compartment $b_p(t)$ and the other compartments of the normalized model are interpreted in different ways in each of the four scenarios, none of the type reproduction numbers ($\mathcal{T}_2^{(j)}$; $j = 1, 2, 3, 4$)) correspond to any of the reproduction numbers $\mathcal{R}_0^{(j)}$ ($j = 1, 2, 3, 4$). Hence, Theorems 4.2 and 4.3 do not automatically hold for Type Reproduction Number $\mathcal{T}_2^{(j)}$ ($j = 1, 2, 3, 4$) corresponding to type 2 population. So in this case, the problem of underestimation or overestimation of the efforts necessary to eliminate the epidemic is not overcome, since in each Scenario, one must act on a different number of cholera particles $b_p(t)$. It is worth noting that, for this population type, the associated type reproduction numbers are not unique. That is, each scenario considered has a type reproduction number that differs from that of the other three scenarios. It should further be stated that, for this population type (i.e., $s = 2$), the minimum threshold coverage needed for *V. cholerae* elimination in the pond is given by $p_2^{(i)} = 1 - \dfrac{1}{\mathcal{T}_2^{(j)}}$ ($j = 1, \cdots, 4$) [5, 34]. Targeting the bacterial population in the pond could correspond to the implementation of a strategy, such as chemical control or water purification, that decreases the bacterial growth in the pond (i.e., reduces r) and increases the bacterial natural mortality rate in the pond (μ_B).

4.3 Targeting population of type 3 (bacteria in the river)

Suppose, now, that a control measure is applied only to population of type 3 (i.e., bacteria in the river). For this case, it follows from Definition (4.1) that the associated vector ($\mathbf{e}_3$) and projection matrix (P_3) are given, respectively, by:

$$\mathbf{e}_3 = \begin{pmatrix}0\\0\\1\end{pmatrix} \text{ and } \quad P_3 = \begin{pmatrix}0&0&0\\0&0&0\\0&0&1\end{pmatrix}. \tag{4.11}$$

Setting $j = 1$, and using $\mathbf{e}_3$, P_3 and the NGM K_1 in Equation (4.1) gives:

$$\mathcal{T}_3^{(1)} = \mathbf{e}_3^T K_1[I - (I - P_3)K_1]^{-1}\mathbf{e}_3 = 0. \tag{4.12}$$

It has already been observed in Section 4.1 that comparing Scenario 1 to the Scenario 2, the assumption (4.2) is satisfied. Moreover, it is easy to see that the hypotheses of the Theorem 4.1 are verified considering the population of type 3 and Scenarios 1 and 2. Since in this case with bacteria in river as the type considered (i.e., $s = 3$), and for all the aforementioned scenarios we compared $s = 3$ always differs from l_1 (with $l_1 = 2$), it follows from Theorem 4.1 that the associated type reproduction number is unique. That is,

$$\mathcal{T}_3^{(1)} = \mathcal{T}_3^{(2)} = 0. \tag{4.13}$$

Indeed, in Scenarios 1 and 2, no new infected bacterial particles are generated in the b_r population. Setting $j = 3$ in Definition (4.1) (together with $\mathbf{e}_3$, P_3 and the NGM K_3) gives:

$$\begin{aligned} \mathcal{T}_3^{(3)} &= \mathbf{e}_3^T K_3[I - (I - P_3)K_3]^{-1}\mathbf{e}_3, \\ &= \frac{V_r\theta_r[\beta_p V_r\lambda_r + k_p\beta_r(\lambda_p + \mu_B - 1)]}{-V_r\beta_p\theta_p a_4 - k_p\beta_r\theta_p\lambda_p + k_p V_r a_3[a_4(\mu_B - 1) + \mu_B\lambda_p]}, \end{aligned} \tag{4.14}$$

provided $\mathcal{T}_3^{(3)} > 0$.

Comparing Scenarios 3 and 4, it is evident, first of all, that Assumption (4.2) holds. In particular (note that $m = 1$ in this case):

$$V_4 = V_3 + U_1, \text{ and } F_4 = F_3 + U_1,$$

where,

$$U_1 = \begin{pmatrix} 0 & 0 & 0 \\ 0 & 1 & 0 \\ 0 & 0 & 0 \end{pmatrix}.$$

In this case, we have $l_1 = 2$ (the second row of U_m (or, equivalently, U_1) corresponds to the compartment b_p, that is interpreted differently). Moreover, it is easy to see that the hypotheses of the Theorem 4.1 are verified considering the population type 3 and Scenarios 3 and 4. Since in this case with bacteria in river as the type considered (i.e., $s = 3$), and for all the aforementioned scenarios we compared $s = 3$ always differs from l_1 (with $l_1 = 2$), it follows from Theorem 4.1 that the associated type reproduction number is unique. That is,

$$\mathcal{T}_3^{(3)} = \mathcal{T}_3^{(4)}. \tag{4.15}$$

Further, none of $\mathcal{T}_3^{(j)}$ (with $j = 1, 2, 3, 4$) coincide with $\mathcal{R}_0^{(j)}$, (with $j = 1, 2, 3, 4$). In other words, the type reproduction numbers $\mathcal{T}_3^{(j)}$ ($j = 1, 2, 3, 4$) cannot be used to establish the local or global asymptotic stability of the disease-free equilibrium, $\mathbf{E}_0$. Furthermore, in this case, if the bacterial population in the river ($b_r(t)$) is reduced by a fraction that exceeds $p_3^{(j)} = 1 - \frac{1}{\mathcal{T}_3^{(j)}}$, with $j = 1, \cdots, 4$, [5] (this can be achieved by implementing strategies that minimize bacterial shedding into the river, for instance, by vaccinating susceptible humans and/or treating cholera-infected humans), the cholera epidemic will die out. Targeting the bacterial population in the river could correspond to the implementation of a control strategy that decreases bacterial abundance in the river (e.g., a chemical control strategy that increases the bacterial natural mortality rate μ_B).

5 Assessment of Control Strategies

In this section, the normalized model (2.3) will be simulated to assess the population-level impact of various anti-cholera control measures. Unless otherwise stated, the numerical simulations will be carried out using the baseline parameter values given in Table 1. Further, the simulations are for the case where the human population is targeted for control (i.e., we are simulating the normalized model for $s = 1$). The values of the various reproduction numbers of the model ($\mathcal{R}_0^{(1)}; i = 1, \cdots, 4$) and herd immunity threshold ($p_s^{(i)}$, with $i = 1, \cdots, 4$ and $s = 1, 2, 3$) are first computed. The results obtained, tabulated in Table 3, show that, for each of the four scenarios, the reproduction number exceeds unity (lying in the range $\mathcal{R}_0^{(i)} \in [2.7, 9.2]$). Hence, in this case (with no anti-cholera intervention implemented in the community), the disease will remain endemic.

Furthermore, this table shows that the amount of effort needed to reduce $\mathcal{T}_1$ to a value less than unity increases with increasing values of $\mathcal{R}_0^{(i)}$. It is also seen that $\mathcal{T}_1^{(i)} = \mathcal{T}_1$, $i = 1, \cdots, 4$ (in line with Equation (4.5)). Moreover, $\mathcal{T}_s^{(1)} = 0$ for $s = 2, 3$, and $\mathcal{T}_3^{(2)} = 0$. This can be explained as follows: In Scenario 1, the bacterial populations in the aquatic environment (b_p and b_r, corresponding to $s = 2$ and $s = 3$, respectively) do not contribute to the generation of new cholera infections (i.e., they do not contribute to the F matrix). Further, in Scenario 2, the population type 3 (i.e., bacteria in the river) does not contribute to the F matrix. Consequently, $p_s^{(1)} = -\infty$ and $p_3^{(2)} = -\infty$. The consequence of this result is that applying an anti-cholera control measure on the population of types $s = 2$ and $s = 3$ in Scenario 1, or on population of type $s = 3$ in Scenario 2, will not lead to the elimination of the disease (this result is consistent with that reported in [5]).

Note also that, if the population of type $s = 2, 3$ is targeted, then none of the associated type reproduction numbers ($\mathcal{T}_s^{(i)}$, $s = 2, 3$, $i = 1, \cdots, 4$) behaves like $\mathcal{R}_0^{(i)}$, $i = 1, \cdots, 4$. In particular, while $\mathcal{T}_s^{(i)} < 1$ for $s = 2$ and $s = 3$, the reproduction numbers $\mathcal{R}_0^{(i)} > 1$ ($i = 1, \cdots, 4$). Hence, when targeting populations of type 2 or 3, the use of type reproduction number (in all four scenarios) does not provide any useful information on the state (endemic or not) of the disease. Further, it does not represent a good estimate of the herd immunity effort needed to eliminate the disease.

Finally, note that, since $\mathcal{R}_0^{(1)} > \mathcal{R}_0^{(2)} > \mathcal{R}_0^{(3)} > \mathcal{R}_0^{(4)}$, it follows that, using $\mathcal{R}_0^{(1)} = \mathcal{T}_1$ as a threshold parameter to eliminate the infection, a greater effort is needed in Scenario 1, in comparison to the effort needed in Scenarios 2, 3 and 4. It is worth mentioning that the above simulations results are sensitive to the values of the bacterial shedding rates into the water environment (θ_p and θ_r). It should be recalled from Table 3 that these parameters are fixed at a baseline value of $\theta_p^* = \theta_r^* = 10^4$ per day. This baseline value is justified as follows. As noted by Feachem et al. [25], it is known that in asymptomatic cases of infection with *V. cholerae*, an individual excrete from 10^2 to 10^5 bacteria per gram of feces, while in symptomatic cases this value can rise to as high as $10^6 - 10^9$ per milliliter of rice-water stool. Further, data from [15] show that a patient with severe cholera infection can produce between 500 to 1000 mL of stool per day (corresponding to 10^{12} *V. cholerae* particles a day, of which a very high fraction (given the reported challenging hygienic conditions prevalent in the area) reaches the water reserve daily).

5.1 Assessment of Single Control Interventions

In this section, the population-level impact of the singular implementation of two anti-cholera interventions, namely a basic control measure and treatment of humans infected with cholera, will be assessed. This is described below.

	Basic Reproductive Number $\mathcal{R}_0$	Target infective host $i(t)$ $(s=1)$	Target bacteria in the pond $b_p(t)$ $(s=2)$	Target bacteria in the river $b_r(t)$ $(s=3)$
Scenario 1	$\mathcal{R}_0^{(1)} = 9.17$ $p^{(1)} = 0.89$	$(\mathcal{T}_1^{(1)} = 9.17)$ $p_1^{(1)} = 0.89$	$(\mathcal{T}_2^{(1)} = 0)$ $p_2^{(1)} = -\infty$	$(\mathcal{T}_3^{(1)} = 0)$ $p_3^{(1)} = -\infty$
Scenario 2	$\mathcal{R}_0^{(2)} = 6.83$ $p^{(2)} = 0.853551$	$(\mathcal{T}_1^{(2)} = 9.17)$ $p_1^{(2)} = 0.89$	$(\mathcal{T}_2^{(2)} = 0.06)$ $p_2^{(2)} < 0$	$(\mathcal{T}_3^{(2)} = 0)$ $p_3^{(2)} = -\infty$
Scenario 3	$\mathcal{R}_0^{(3)} = 3.03$ $p^{(3)} = 0.67$	$(\mathcal{T}_1^{(3)} = 9.17)$ $p_1^{(3)} = 0.89$	$(\mathcal{T}_2^{(3)} = 0.86)$ $p_2^{(3)} < 0$	$(\mathcal{T}_3^{(3)} < 0)$ $p_3^{(3)} > 1$
Scenario 4	$\mathcal{R}_0^{(4)} = 2.7$ $p^{(4)} = 0.63$	$(\mathcal{T}_1^{(4)} = 9.17)$ $p_1^{(4)} = 0.89$	$(\mathcal{T}_2^{(4)} < 0)$ $p_2^{(4)} > 1$	$(\mathcal{T}_3^{(4)} < 0)$ $p_3^{(4)} > 1$

Table 3: Basic reproduction numbers ($\mathcal{R}_0^{(i)}$; $i = 1, \cdots, 4$), type reproduction numbers ($\mathcal{T}_s^{(i)}$; $i = 1, \cdots, 4$; $s = 1, 2, 3$) and herd immunity thresholds ($p_s^{(i)}$; $i = 1, \cdots, 4$; $s = 1, 2, 3$) for the normalized model (2.3). Parameter values used are as given by the baseline values in Table 1.

5.1.1 Basic anti-Cholera control measures (WASH-only strategy)

Basic anti-cholera control entail the use of measures aimed at preventing or mitigating cholera outbreak in the community. These measures typically include the implementation of the water, sanitation and hygiene (WASH) strategy [26]. The essential elements of the WASH strategy include the chlorination of water sources, household water treatment and the promotion of personal hygienic precautions, use of chemical insecticides, etc. Hence, in the context of the normalized model, the implementation of basic control measures will be associated with strategies that decrease the transmission rates (β_p and β_r) and increase the *V. cholerae* decay (natural death) rate (μ_B). This is obtained by making the following replacements in the model:

$$\begin{aligned} \beta_p &\to \beta_p\,(1-\varepsilon_B c_B)\,, \\ \beta_r &\to \beta_r\,(1-\varepsilon_B c_B)\,, \\ \mu_B &\to \mu_B\,(1+\varepsilon_B c_B)\,, \end{aligned} \tag{5.1}$$

where $0 \leq \varepsilon_B \leq 1$ and $0 \leq c_B \leq 1$ represent, respectively, the efficacy and coverage of the WASH-only control strategy. Although a clear consensus on the realistic estimate of the efficacy and/or coverage of the basic control measures in cholera-endemic areas seems to be lacking, a number of studies have provided some clues as to what these estimates should be. For instance, in a modeling study on assessing the impact of WASH and oral cholera vaccine on the 2008 cholera epidemic in Haiti, Fung et al. [26] reported that (in 2008) only 63% of the Haitian population had access to improved water and only 17% had access to improved sanitation. Furthermore, after the 2010 earthquake in Haiti, the Haitian Directorate for Potable Water and Sanitation reported that 26% of the rural population received improved water, while only 10% had improved sanitation (in particular, the coverage for improved water and sanitation in the urban

Port-au-Prince metropolitan area was 35% and 20%, respectively). Fung et al. [26] introduced non-linear relationships between coverage and effectiveness of the aforementioned interventions. Based on all these, it seems reasonable to assume that the WASH coverage lies in the range 30% and 50%, while its efficacy can be anywhere between 10% and 60%.

Replacing β_p, β_r and μ_B in the normalized model (2.3) with the expressions in (5.1), it follows that the associated basic type reproduction number (defined in (4.5)) now becomes (with $i = 1, \cdots, 4$):

$$\begin{aligned}\mathcal{T}_{1B} &= \mathcal{T}_{1B}^{(i)} = \mathcal{R}_{0B}{}^{(1)} \\ &= \frac{V_r\beta_p(1-\varepsilon_B c_B)a_{1B} + k_p\beta_r(1-\varepsilon_B c_B)\left[(\theta_p + V_r\theta_r)\lambda_p + V_r\theta_r(\mu_B(1+\varepsilon_B c_B)-1)\right]}{k_p V_r a_3[(\lambda_r + \mu_B(1+\varepsilon_B c_B))(\mu_B(1+\varepsilon_B c_B)-1) + \mu_B(1+\varepsilon_B c_B)\lambda_p]},\end{aligned}$$

where,

$$a_{1B} = V_r\theta_r\lambda_r + \theta_p(\lambda_r + \mu_B(1+\varepsilon_B c_B)).$$

Thus, the associated threshold herd immunity threshold becomes: $p_{1B}^{(i)} = 1 - \dfrac{1}{\mathcal{T}_{1B}}$ $(i = 1, \cdots, 4)$, with $\mathcal{T}_{1B}$ defined in (5.2).

For simulation purposes, the following effectiveness levels of the basic control measures (based on reducing β_p and β_r and increasing μ_B, in comparison to the baseline values of the respective non-normalazed parameters tabulated in Table 1) are considered:

1. **Low effectiveness level of WASH-only strategy**: involves reducing the baseline values of b_p and b_r by 10% (i.e., $\beta_p = \beta_r = 15$, $\beta_p^* = \beta_r^* = 4.5$), and increasing the baseline value of μ_B by 10% (i.e., $\mu_B = 2,93$, $\mu_B^* = 0.88$).

2. **Moderate effectiveness level of WASH-only strategy**: involves reducing the baseline values of b_p and b_r by 25% (i.e., $\beta_p = \beta_r = 12.5$, $\beta_p^* = \beta_r^* = 3.75$) and increasing the baseline value of μ_B by 25% (i.e., $\mu_B = 3.33$, $\mu_B^* = 1$).

3. **High effectiveness level of WASH-only strategy**: involves reducing the baseline values of b_p and b_r by 50% (i.e., $\beta_p = \beta_r = 8.33$, $\beta_p^* = \beta_r^* = 2.5$) and increasing the baseline value of μ_B by 50% (i.e., $\mu_B = 4$, $\mu_B^* = 1.2$).

Figure 6 depicts the contour plots of $\mathcal{R}_{0B}{}^{(1)} = \mathcal{T}_{1B}$ (defined in (5.2)), as a function of efficacy (ε_B) and coverage (c_B) of the basic anti-cholera control measures for the low, moderate and high effectiveness levels. It follows from this figure ((a)) that even with the highest possible estimated efficacy and coverage of the basic control measure (i.e., $\varepsilon_B = 0.6$ and $c_B = 0.5$), none of the effectiveness levels of this basic control strategy can lead to the elimination of the disease (albeit each will greatly decrease the disease burden). The reason is that, with efficacy at 60% and coverage at 50%, none of the effectiveness levels can bring the associated reproduction number to a value less than unity regardless of the level of coverage. If, however, the efficacy of the basic control measure can be dramatically increased to 90%, then both the moderate and high effectiveness levels of this strategy can lead to such elimination if the coverage level is high enough (at least 80%) (Figures (b) and (c)). If the efficacy and coverage can further be increased to 100% each (the study in Fung et al. [26] showed that 100% coverage is possible, over a 20-year period, in urban areas of Haiti), then low effectiveness level can also achieve such elimination (Figure (a)).

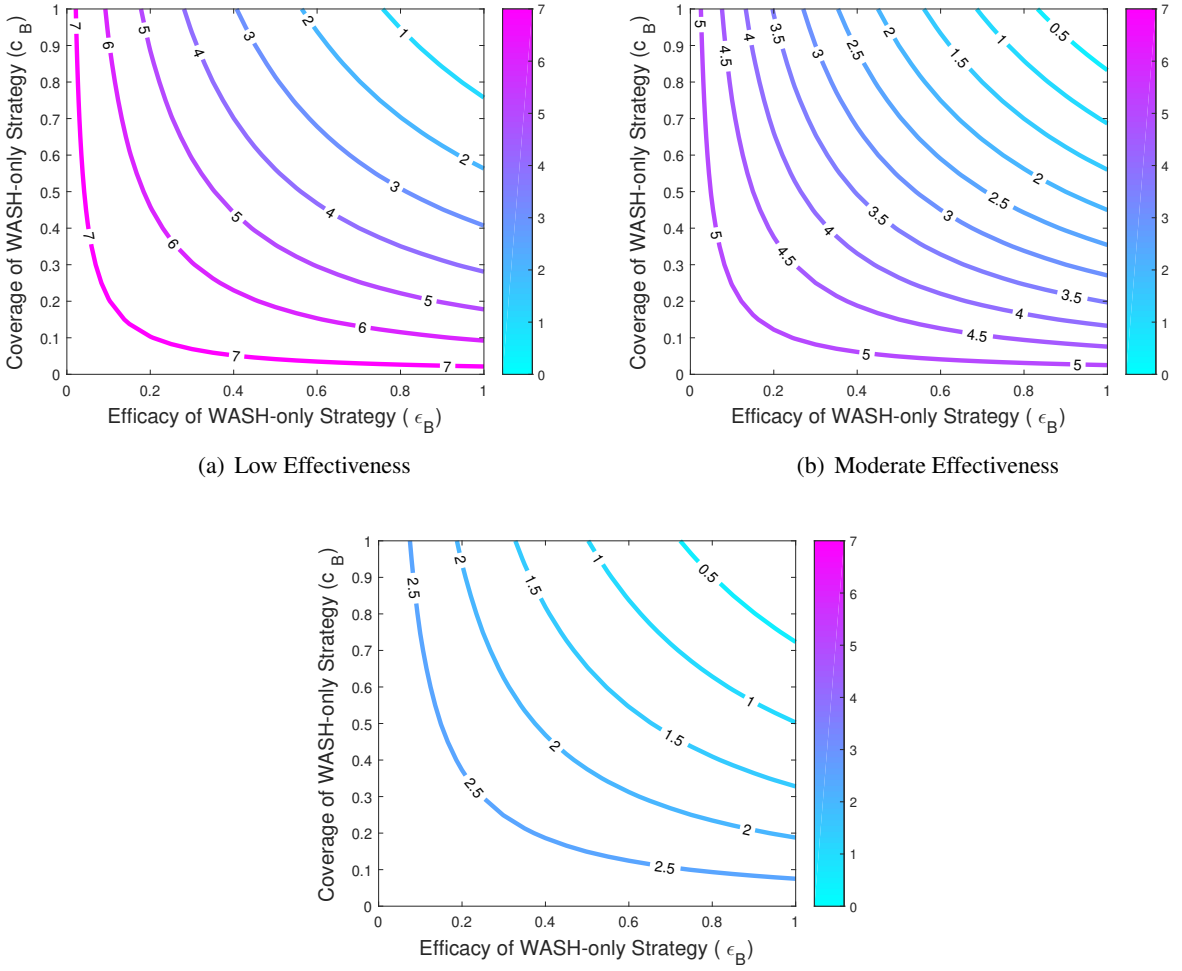

(a) Low Effectiveness

(b) Moderate Effectiveness

(c) High Effectiveness

Figure 6: Simulations of the model (2.3) with low (a), moderate (b) and high (c) effectiveness level of the WASH-only strategy. Contour plot of $\mathcal{R}_{0B}{}^{(1)}$ as a function of efficacy ε_B and coverage c_B. Parameter values used are as given in Table 1, with a reduction (increase) of the value of parameters β_p^* and β_r^* (μ_B^*) by: (a) 10%, (b) 25% (b) and (c) 50%, in comparison to their baseline values given in Table 1.

5.1.2 Treatment-only strategy

In this section, a treatment-only strategy, targeting infected humans, is considered. Cholera can be successfully treated, in most cases, using oral rehydration therapy [68, 48]. Although recovery from cholera infection is feasible without taking antibiotics (if sufficient hydration is maintained) [68, 48], the WHO recommends the use of antibiotic treatments (for one to three days), aimed at reducing the severity of the disease symptoms [68, 48]. In particular, in patients with severe dehydration [68, 48], *Doxycycline* is typically used as a first line drug (although some strains of *V. cholerae* have shown resistance to it [53]). Other antibiotics that have been proven to be effective againts *V. cholerae* infection include *cotrimoxazole, erythromycin, tetracycline, chloramphenicol*, and *furazolidone* [68, 48]. Furthermore, *Fluoroquinolones*, such as *ciprofloxacin*, may be used (but the ability of *V. cholerae* to resist the effects of this substance has also been reported in [36]). The use of antibiotics also reduces the need for fluid replacement therapy. It is known that zinc supplementation reduces the duration and severity of diarrhea in Bangladeshi children with cholera when given in combination with antibiotics and rehydration therapy as needed (in particular,

it reduced the duration of the disease (i.e., duration of cholera-related diarrheal illness) by eight hours, in addition to reducing the amount of diarrhea stool by 10% [68, 48]).

The use of treatment against *V. cholerae* infection in the community affects the parameters related to the shedding of bacteria by humans and the recovery of those who contracted the disease. In particular, the use of treatment decreases the shedding rate parameters (θ_p and θ_r), while increasing the recovery parameter (γ). Consequently, the treatment-only strategy is incorporated into the normalized model by replacing the three associated parameters as follows:

$$\begin{aligned} \theta_p &\to \theta_p(1-\varepsilon_T c_T), \\ \theta_r &\to \theta_r(1-\varepsilon_T c_T), \\ \gamma &\to \gamma(1+\varepsilon_T c_T), \end{aligned} \tag{5.2}$$

where ε_T and c_T are, respectively, the efficacy and coverage of the treatment-only strategy. Using data for cholera epidemics in Bangladesh from 1985-1991, Siddique et al. [60] estimated that only 20% of cholera-infected people were treated in government health facilities (with 80% of the infected population treated at home). Furthermore, only about 23% of the cholera-infected people were actually treated by qualified physicians (with 68% of the infected individuals treated by unqualified rural practitioners and 9% had no access to any health care providers). Sack et al. [54] reported that rehydration treatment (which is inexpensive and simple to implement) is approximately 100% successful (or effective).

Replacing θ_p, θ_r and γ in the normalized model (2.3) with the expressions in (5.2), it follows that the associated basic type reproduction number (defined in (4.5)) now becomes (with $i = 1, \cdots, 4$):

$$\begin{aligned} \mathcal{T}_{1T} &= \mathcal{T}_{1T}^{(i)} = \mathcal{R}_{0T}{}^{(1)} \\ &= \frac{V_r\beta_p a_{1T} + k_p\beta_r\left[(\theta_p(1-\varepsilon_T c_T) + V_r\theta_r(1-\varepsilon_T c_T))\lambda_p + V_r\theta_r(1-\varepsilon_T c_T)(\mu_B-1)\right]}{k_p V_r a_{3T}[a_4(\mu_B-1)+\mu_B\lambda_p]}, \end{aligned}$$

where,

$$a_{1T} = V_r\lambda_r\theta_r(1-\varepsilon_T c_T) + \theta_p(1-\varepsilon_T c_T)(\lambda_r+\mu_B),$$
$$a_{3T} = \gamma(1+\varepsilon_T c_T) + \delta + \mu.$$

Thus, the associated herd immunity threshold becomes: $p_{1T}^{(i)} = 1 - \dfrac{1}{\mathcal{T}_{1T}}$ $(i = 1, \cdots, 4)$, with $\mathcal{T}_{1T}$ defined in (5.3).

As before, we consider the following effectiveness levels of the treatment-only strategy (based on reducing θ_p and θ_r and increasing γ, in comparison to the baseline values of the respective non-normalized parameters tabulated in Table 1):

1. **Low effectiveness level of treatment-only strategy**: involves reducing the baseline values of θ_p and θ_r by 10% (i.e., $\theta_p = \theta_r = 3\times 10^4$, $\theta_p^* = \theta_r^* = 9\times 10^3$), and increasing the baseline value of γ by 10% (i.e., $\gamma = 0.73$, $\gamma^* = 0.22$).

2. **Moderate effectiveness level of treatment-only strategy**: involves reducing the baseline values of θ_p and θ_r by 25% (i.e., $\theta_p = \theta_r = 2.5\times 10^4$, $\theta_p^* = \theta_r^* = 7.5\times 10^3$) and increasing the baseline value of γ by 25% (i.e., $\gamma = 0.83$, $\gamma^* = 0.25$).

3. **High effectiveness level of treatment-only strategy**: involves reducing the baseline values of θ and θ_r by 50% (i.e., $\theta_p = \theta_r = 1.6666\times 10^4$, $\theta_p^* = \theta_r^* = 5\times 10^3$) and increasing the baseline value of γ by 50% (i.e., $\gamma = 1$, $\gamma^* = 0.3$).

Figure 7 depicts the contour plots of $\mathcal{R}_{0T}{}^{(1)} = \mathcal{T}_{1T}$ (defined in (5.3)), as a function of efficacy (ε_T) and coverage (c_T) of the treatment-only strategy for the low, moderate and high effectiveness levels of the treatment-only strategy. It follows from Figure 7 that, with the 23% anti-cholera treatment coverage, cholera elimination is not feasible no matter the efficacy level of the treatment used (this is because the associated reproduction number remains above unity when $c_T = 0.23$ and $\varepsilon_T = 1$). However, if the coverage can be significantly increased to at least 80%, this figure shows that even the low effectiveness level of this strategy can lead to the elimination of the disease (requiring a treatment efficacy of at least 100%). Furthermore, such elimination can be achieved if the coverage is lowered to 70% using the moderate effectiveness level of the treatment strategy (here, a minimum treatment efficacy of 100% would be needed). Finally, for 50% treatment coverage, the high effectiveness level of the treatment-only strategy can lead to disease elimination if its efficacy is at least 100%. In summary, these simulations suggest that a highly-effective treatment-only strategy (with efficacy of at least 100%) can lead to the elimination of cholera if a modest coverage level (of at least 50% can be attained and maintained).

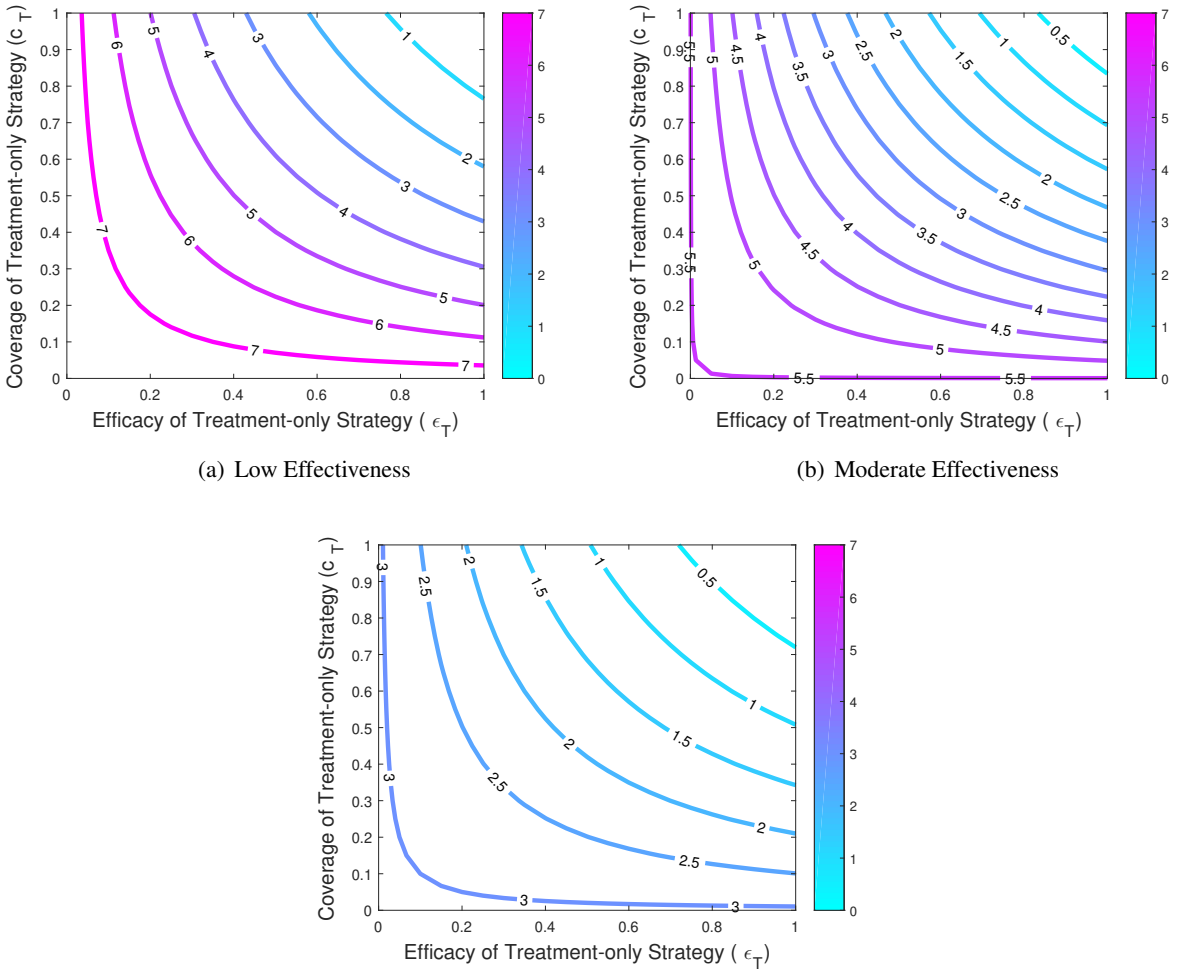

(a) Low Effectiveness

(b) Moderate Effectiveness

(c) High Effectiveness

Figure 7: Simulations of the model (2.3) with low (a), moderate (b) and high (c) effectiveness level of the treatment-only strategy. Contour plot of $\mathcal{R}_{0T}{}^{(1)}$ as a function of efficacy ε_T and coverage c_T. Parameter values used are as given in Table 1, with a reduction (increase) of the value of parameters θ_p^* and θ_r^* (γ^*) by: (a) 10%, (b) 25% and (c) 50%, in comparison to their baseline value given in Table 1.

5.2 Assessment of Combined WASH-Treatment Strategy

In this section, the population-level impact of a hybrid strategy that combines both the WASH-only and the treatment-only strategy will be assessed. The essential elements of the combined strategy include a reduction in both the transmission and shedding rates, in addition to an increase in both the natural bacterial death rate and the recovery rate for humans. For this strategy, the associated parameters β_p, β_r, θ_p, θ_r, μ_B and γ are replaced by the following relations:

$$\begin{aligned} \beta_p &\to \beta_p(1-\varepsilon_{BT}c_{BT}), \quad \theta_p \to \theta_p(1-\varepsilon_{BT}c_{BT}), \\ \beta_r &\to \beta_r(1-\varepsilon_{BT}c_{BT}), \quad \theta_r \to \theta_r(1-\varepsilon_{BT}c_{BT}), \\ \mu_B &\to \mu_B(1+\varepsilon_{BT}c_{BT}), \quad \gamma \to \gamma(1+\varepsilon_{BT}c_{BT}), \end{aligned} \tag{5.3}$$

where ε_{BT} and c_{BT} are efficacy and coverage of combined WASH-treatment strategy.

Replacing β_p, β_r, θ_p, θ_r μ_B and γ in the normalized model (2.3) with the expressions in (5.3), it follows that the associated basic type reproduction number (defined in (4.5)) now becomes (with $i = 1, \cdots, 4$):

$$\begin{aligned} \mathcal{T}_{1BT} &= \mathcal{T}_{1BT}^{(i)} = {\mathcal{R}_{0BT}}^{(1)} \\ &= \frac{V_r\beta_p(1-\varepsilon_{BT}c_{BT})a_{1BT} + k_p\beta_r(1-\varepsilon_{BT}c_{BT})a_7}{k_pV_ra_{3BT}[a_4(\mu_B(1+\varepsilon_{BT}c_{BT})-1)+\mu_B(1+\varepsilon_{BT}c_{BT})\lambda_p]}, \end{aligned}$$

where,

$$a_{1BT} = V_r\lambda_r\theta_r(1-\varepsilon_{BT}c_{BT}) + \theta_p(1-\varepsilon_{BT}c_{BT})(\lambda_r+\mu_B(1+\varepsilon_{BT}c_{BT})),$$

$$a_{3BT} = \gamma(1+\varepsilon_Tc_T)+\delta+\mu,\ a_4 = \lambda_r+\mu_B(1+\varepsilon_{BT}c_{BT}),$$

$$a_7 = (\theta_p(1-\varepsilon_{BT}c_{BT}) + V_r\theta_r(1-\varepsilon_{BT}c_{BT}))\lambda_p + V_r\theta_r(1-\varepsilon_{BT}c_{BT})(\mu_B(1+\varepsilon_{BT}c_{BT})-1).$$

Thus, the corresponding threshold herd immunity becomes $p_{1BT}^{(i)} = 1 - \frac{1}{\mathcal{T}_{1BT}}$, with $\mathcal{T}_{1BT}$ defined in (5.4). We estimate the coverage and efficacy of this strategy by taking, for example, the mean of the coverages and efficacies of the WASH-only and treatment-only strategies. That is, $\varepsilon_{BT} = (\varepsilon_B+\varepsilon_T)/2 = (0.6+1)/2 = 0.8$ and $c_{BT} = (c_B + c_T)/2 = (0.5 + 0.23)/2 = 0.365$.

We consider the following effectiveness levels of the combined strategy

1. **Low effectiveness level of combined WASH-treatment strategy**: involves reducing the baseline values of β_p, β_r, θ_p and $\theta_r$by 10% (i.e., $\beta_p = \beta_r = 15$, $\beta_p^* = \beta_r^* = 4.5$, $\theta_p = \theta_r = 3\times10^4$, $\theta_p^* = \theta_r^* = 9\times10^3$), and increasing the baseline value of μ_B and γ by 10% (i.e., $\mu_B = 2.93$, $\mu_B^* = 0.88$, $\gamma = 0.73$, $\gamma^* = 0.22$).

2. **Moderate effectiveness level of combined WASH-treatment strategy**: involves reducing the baseline values of β_p, β_r, θ_p and θ_r by 25% (i.e. $\beta_p = \beta_r = 12.5$, $\beta_p^* = \beta_r^* = 3.75$, $\theta_p = \theta_r = 2.5\times10^4$, $\theta_p^* = \theta_r^* = 7.5\times10^3$) and increasing the baseline value of μ_B and γ by 25% (i.e., $\mu_B = 3.33$, $\mu_B^* = 1$ and $\gamma = 0.83$, $\gamma^* = 0.25$).

3. **High effectiveness level of combined WASH-treatment strategy**: involves reducing the baseline values of β_p, β_r, θ_p and θ_r by 50% (i.e.,$\beta_p = \beta_r = 8.33$, $\beta_p^* = \beta_r^* = 2.5$, $\theta_p = \theta_r = 1.6666\times10^4$, $\theta_p^* = \theta_r^* = 5\times10^3$) and increasing the baseline value of μ_B and γ by 50% (i.e.,$\mu_B = 4$, $\mu_B^* = 1.2$ and $\gamma = 1$, $\gamma^* = 0.3$).

Figure 7 depicts the contour plots of $\mathcal{R}_{0BT}{}^{(1)} = \mathcal{T}_{1BT}$ (defined in (5.3)), as a function of efficacy (ε_{BT}) and coverage (c_{BT}) of the treatment strategy for the low, moderate and high effectiveness levels. This figure shows that the high effectiveness level of this (combined) strategy will lead to cholera elimination even for sufficiently small coverage and efficacy (Figure 8(c)). For the aforementioned 80% efficacy and 36.5% coverage assumed for this strategy, it is shown that neither the low or moderate effectiveness level of this intervention can lead to disease elimination. However, if the coverage is increased to 50%, even the low effectiveness level of this intervention can lead to cholera elimination (Figure 8(a)). The moderate effectiveness level at 80% efficacy can lead to elimination with even a 40% coverage (Figure 8(b))). Thus, it can be concluded that the combined strategy offers the best prospect for cholera elimination in the community (since it requires the lowest minimum coverage needed to achieve such elimination). In summary, this study ranks the three interventions (in order of their effectiveness, *vis a vis* their ability to lead to cholera elimination) as follows:

$$\boxed{\text{Combined Strategy} > \text{Treatment-only Strategy} > \text{WASH-only Strategy}}.$$

6 Discussion and Conclusions

Cholera, a water-borne disease characterized by severe diarrhea, remains a major public health burden in many parts of the world. In particular, the disease, caused by *Vibrio cholerae*, is endemic in parts of Asia, Africa, and Latin America. Owing to the enormous public health burden associated with cholera disease, there is now a concerted global effort to effectively control and/or eliminate the disease in endemic areas. In particular, the Global Task Force on Cholera Control (GTFCC) has launched a laudable collaborative initiative in 2017 with the dual aim of reducing cholera mortality by 90% in the existing 47 countries affected by cholera and, subsequently, ending cholera as a threat to public health by 2030 [46]. The essential elements of the laudable GTFCC initiative include intensifying anti-cholera control efforts (in particular improved WASH strategy, safe drinking water, quick access to treatment, intravenous fluids and antibiotic for severe cholera cases), enhancing preparedness of health case systems and building strong capacity to effectively and rapidly contain cholera outbreaks [46]. The aforementioned global effort to eliminate cholera necessitate the design and use of novel mathematical modeling framework for gaining insight into cholera transmission dynamics and control, aimed at finding effective strategies for achieving cholera elimination (*vis a vis* the 2030 elimination goal).

In this paper, a novel ecology-epidemiology-hydrology model for the environment-host-environment transmission dynamics and control of *V. cholerae* bacteria in a human host population having an interconnected pond-river water network is proposed. The model, which takes the form of a deterministic system of nonlinear differential equations, accounted for the back-and-forth flow of water within the pond-river network. Further, the model stratified the total bacterial population in the aquatic environment based on which of the two water bodies the bacteria reside in. That is, the total bacterial population is split into sub-population for bacteria in the pond and bacteria in the river. Other notable features of the novel model include the use of a nonlinear logistic growth rate for bacteria in the pond (and no such growth is considered for *V. cholerae* dynamics in the river) and accounting for the temporal evolution of the volume of water in the pond (to account for the impact of environmental factors, such as drainage, precipitation, evaporation etc., on *V. cholerae* concentration in the pond). Humans acquire *V. cholerae* infection by coming in contact with contaminated water in either the pond or river, and infected humans shed *V. cholerae* to the two water sources (thereby completing the environment-host-environment cholera transmission cycle).

The developed model was rigorously analysed to gain insight into its dynamical features. In particular, results for the non-negativity, invariance and boundedness of the model were derived (thereby establishing the well-posedness of the developed model). The asymptotic stability of the disease-free equilibrium of the

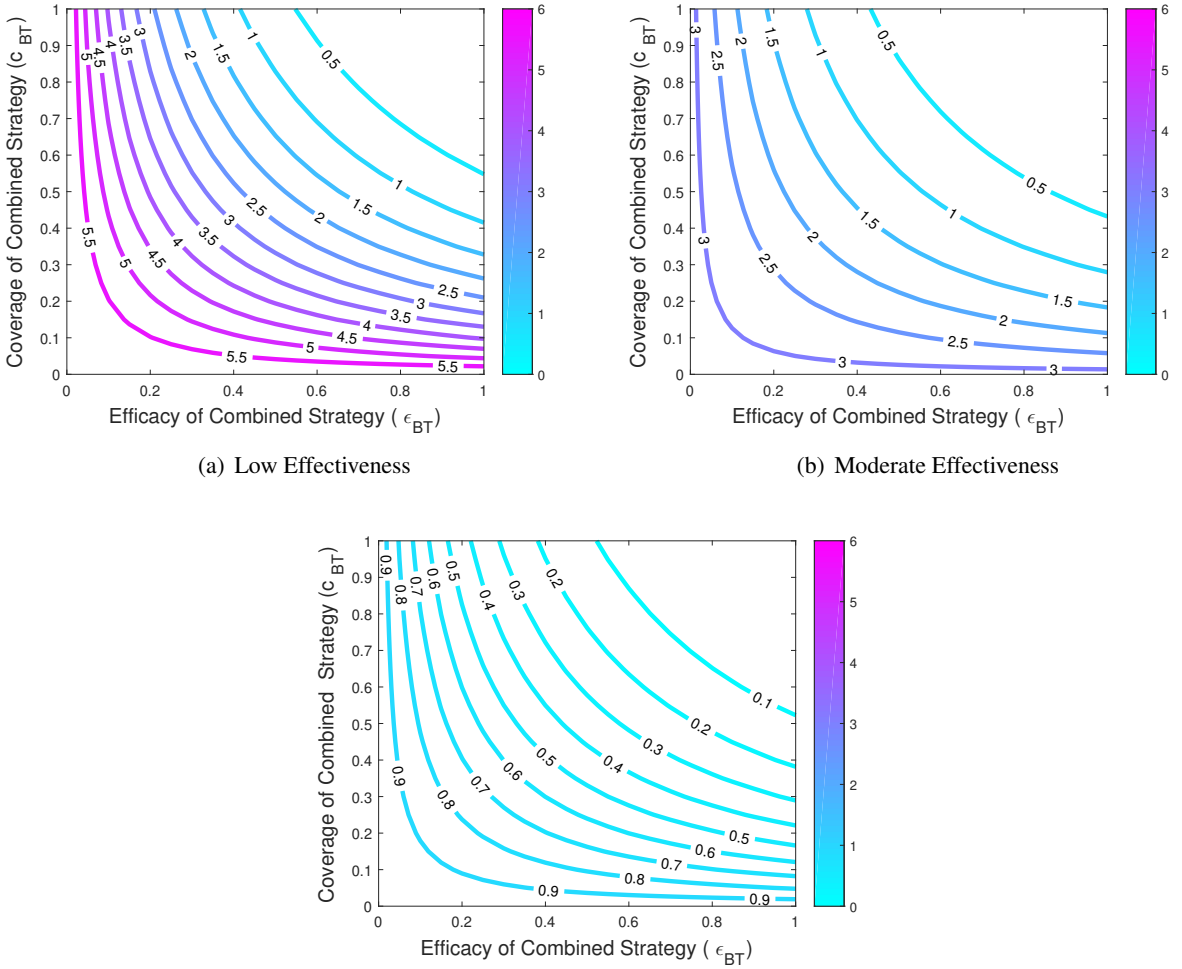

(a) Low Effectiveness

(b) Moderate Effectiveness

(c) High Effectiveness

Figure 8: Simulations of the model (2.3) with low (a), moderate (b) and high (c) effectiveness level of the hybrid strategy. Contour plot of $\mathcal{R}_0^{(1)}$ as a function of efficacy ε_{BT} and coverage c_{BT}. Parameter values used are as given in Table 1, with a reduction (increase) of the value of parameters β_p^*, β_r^*, θ_p^* and θ_r^* (γ^* and μ_B^*) by: (a) 10%, (b) 25% and (c) 50%, in comparison to their baseline values given in Table 1.

model was shown to be governed by whether or not a certain epidemiological threshold, known as the basic reproduction number (denoted by $\mathcal{R}_0$), is less than unity. Explicit expressions for $\mathcal{R}_0$ of the developed model were derived under four different anti-cholera control scenarios. The four control scenarios were formulated based on using four different interpretations of the role of the environment in the transmission cycle.

For the special case of the model where the bacterial growth is less than the bacterial death, it was shown that all the four expressions of $\mathcal{R}_0$ are well-posed. Further, the four constituent reproduction numbers exhibit the same threshold property with respect to the value unity (i.e., if one is less(equal)(greater) than unity, then the remaining three are all less(equal)(greater) than unity). In this context, each control scenario is associated with its own (different) threshold quantity that governs its effectiveness *vis a vis* disease elimination or persistence (i.e., each constituent reproduction number is associated with the amount of effort, in terms of the associated *herd immunity* threshold, needed for the elimination of the disease). In order to overcome the problem of having to deal with different estimates of the effort needed to eliminate the disease corresponding to each of the aforementioned four scenarios considered, the associated *type reproduction number* [5, 30,

52, 58, 59] of the model was computed for each of the three populations type considered in the study (i.e., humans, pond and river). For the case where control efforts exclusively target the human host population, it was shown that the associated type reproduction number (denoted by $\mathcal{T}_1$) was precisely the same for each of the four control scenarios. The uniqueness of the target reproduction when the human hosts are targeted (which plays a critical role in disease control) was, however, not maintained when the other two population types (bacteria in pond and river) are targeted. It should be recalled from the computations in Section 3 that the entries of the first row of the matrix F, of new infection terms, remain the same regardless of which of the four transmission scenarios is considered. Thus, mathematically-speaking (in line with Theorem 4.1), targeting the population type corresponding to the first row of the matrix F (i.e., the human host) guarantees the uniqueness of the associated type reproduction number ($\mathcal{T}_1$). Biologically-speaking, the type reproduction number is unique if it corresponds to a population type that always assumes the same epidemiological role in every scenario. In fact, targeting the bacterial population in the aquatic environment (i.e., in the pond and/or in the river), the corresponding type reproduction number is not unique. This is owing to the fact that the two population types (i.e., bacteria in the pond and in the river) assume different epidemiological roles depending on the transmission scenario considered.

Using Lypapunov function theory and LaSalle's Invariance Principle, it was shown that, for each of the four control scenarios considered, the disease-free equilibrium of the model is globally-asymptotically stable, for a special case where the volume of water in the pond is maximized, whenever the associated reproduction number of the model ($\mathcal{R}_0$; or, equivalently, $\mathcal{T}_1$) is less than unity. The epidemiological implication of this result is that cholera elimination can be achieved if the anti-cholera control strategies adopted can bring (and maintain) $\mathcal{R}_0$ (or $\mathcal{T}_1$) to a value less than unity. Mathematically-speaking, this result means that bringing (and maintaining) $\mathcal{R}_0$ (or $\mathcal{T}_1$) to a value less than unity is necessary and sufficient for the elimination of the disease. This result enabled the determination of the herd immunity threshold (i.e., the minimum proportion of the population that should be targeted for the control) needed for disease elimination.

The developed model was used to assess various effectiveness levels of singular and combined anti-cholera control strategies. In particular, three strategies, namely WASH-only, treatment-only and combined WASH-treatment strategies were considered. Further, for each of these strategies, three effectiveness levels (low, moderate and high) were considered in the numerical simulations of the developed model. Extensive numerical simulations of the model, using reasonably-realistic set of parameters obtained from the literature, showed that, with its current estimated efficacy (of 60%) and coverage (of 50%) [26], the WASH-only strategy (i.e., a strategy that focus on improved water, sanitation and hygiene) is unable to lead to the elimination of cholera in the community, regardless of the effectiveness level (since none of its three effectiveness levels can bring $\mathcal{R}_0$ to a value less than unity). However, our simulations show that such elimination can be achieved, using either the moderate or high effectiveness level of this singular strategy, if the coverage can be increased to 80% and efficacy of implementation greatly increased to 90%. This may not be realistic targets in resource-challenged communities.

For the treatment-only strategy (i.e., a strategy based on using oral rehydration therapy and the administration of antibiotics), it was also shown that, with the current estimate of efficacy and coverage at 100% and 23%, respectively [26, 53, 60], none of the effectiveness levels of this singular strategy can to cholera elimination. Such elimination will, however, be achieved, using even the low effectiveness level, if the coverage can be increased to 80%. In fact, while the implementation of the moderate effectiveness level of this strategy can lead to such elimination with reduced coverage of 70%, the high effectiveness level of this treatment-only strategy can lead to disease elimination even with 50% coverage. Thus, our simulations suggest that treatment-based interventions may be more effective than WASH-based interventions. It is probably plausible to surmise that treatment-based interventions may be more realistic (i.e., achieve the required efficacy and coverage) than WASH-based interventions, particularly in resource-challenged rural areas.

Simulations of the model for the combined (hybrid) WASH-treatment strategy showed that, with the

estimated efficacy of 80% and coverage of 36.5% [53, 60], while the low and moderate effectiveness levels of this hybrid strategy failed to eliminate the disease, the high effectiveness level of this strategy can eliminate the disease. If the coverage is increased to 50%, even the low effectiveness level of this intervention can lead to cholera elimination (in fact, the moderate effectiveness level can achieve such elimination even with a 40% coverage). Hence, it can be concluded, based on our extensive numerical simulations, that the anti-cholera control strategies considered in this study can be ranked in the following order of population-level effectiveness:

$$\boxed{\text{Combined Strategy} > \text{Treatment-only Strategy} > \text{WASH-only Strategy}}.$$

In summary, this study shows that the prospect of effective control or elimination of cholera is promising using reasonably-attainable effectiveness levels and coverage of the currently-available singular control (WASH-only and treatment-only) and their combination.

Acknowledgments

Two of the authors (AL and AP) acknowledges the support of Gruppo Nazionale per la Fisica Matematica (GNFM) and The Istituto Nazionale di Alta Matematica Francesco Severi (INdAM) of Italy. One of the authors (ABG) acknowledge the support, in part, of the Simons Foundation (Award #585022) and the National Science Foundation (Award 1917512). The authors are grateful to the three anonymous reviewers for their very constructive comments.

Appendix A

A1: Proof of Routh-Hurwitz Condition for the Cubic in Equation (3.5)

It should be recalled from Equation (3.6) that the coefficient, b_1, is given by:

$$b_1 = (a_3 + a_4)(\mu_B - 1) + a_3(a_4 + \lambda_p) + \mu_B\lambda_p - \beta_r\theta_r - \frac{\beta_p\theta_p}{k_p},$$

which can be re-written as:

$$b_1 = a_4(\mu_B - 1) + \lambda_p\mu_B + a_3(a_4 + \lambda_p + \mu_B - 1) - \frac{\beta_p\theta_p V_r\mu_B + \beta_r\theta_r k_p V_r\mu_B}{k_p V_r\mu_B}. \tag{A-1}$$

Further, it follows from Equation (3.4) that:

$$\begin{aligned}\beta_p\theta_p V_r\mu_B + \beta_r\theta_r k_p V_r\mu_B &= \mathcal{R}_0^{(1)} a_3 k_p V_r[a_4(\mu_B - 1) + \lambda_p\mu_B] - V_r\beta_p[V_r\theta_r\lambda_r + \theta_p\lambda_r] \\ &- k_p\beta_r[\theta_p\lambda_p + V_r\theta_r(\lambda_p - 1)].\end{aligned} \tag{A-2}$$

Substituting (A-2) into (A-1) gives:

$$\begin{aligned}b_1 &= \frac{1}{k_p V_r\mu_B}\{a_3 k_p V_r\mu_B(a_4 + \lambda_p)\left(1 - \mathcal{R}_0^{(1)}\right) + (a_4 + a_3)\, k_p V_r\mu_B(\mu_B - 1) \\ &+ k_p V_r\left(\mu_B^2\lambda_p + a_3 a_4\mathcal{R}_0^{(1)}\right) + V_r\beta_p(V_r\theta_r\lambda_r + \theta_p\lambda_r) \\ &+ k_p\beta_r[\theta_p\lambda_p + V_r\theta_r(\lambda_p - 1)]\}.\end{aligned} \tag{A-3}$$

Recalling the assumption $\lambda_p \geq 1$, it then follows from (A-3) that $b_1 > 0$ whenever $\mathcal{R}_0^{(1)} < 1$. Thus, the associated Routh-Hurwitz condition, $b_1 b_2 - b_0$, can be re-written as:

$$\begin{aligned}b_2 b_1 - b_0 &= \frac{a_3 + a_4 + \lambda_p + \mu_B - 1}{k_p V_r\mu_B}\{a_3 k_p V_r\mu_B(a_4 + \lambda_p)\left(1 - \mathcal{R}_0^{(1)}\right) \\ &+ (a_4 + a_3)\, k_p V_r\mu_B(\mu_B - 1) + k_p V_r\left(\mu_B^2\lambda_p + a_3 a_4\mathcal{R}_0^{(1)}\right) \\ &+ V_r\beta_p(V_r\theta_r\lambda_r + \theta_p\lambda_r) + k_p\beta_r[\theta_p\lambda_p + V_r\theta_r(\lambda_p - 1)]\} \\ &- a_3[a_4(\mu_B - 1) + \lambda_p\mu_B]\left(1 - \mathcal{R}_0^{(1)}\right) \\ &> 0.\end{aligned} \tag{A-4}$$

Hence, it follows from (A-4) and the expressions for the coefficients b_2 and b_0 in (3.6), that the Routh-Hurwitz condition $b_2 b_1 - b_0 > 0$ if and only if:

$$\begin{aligned}&\{(a_3 + a_4 + \lambda_p + \mu_B - 1)a_3(a_4 + \lambda_p) - a_3[a_4(\mu_B - 1) + \lambda_p\mu_B]\}\left(1 - \mathcal{R}_0^{(1)}\right) \\ > \; &-\frac{a_3 + a_4 + \lambda_p + \mu_B - 1}{k_p V_r\mu_B}\{(a_4 + a_3)\, k_p V_r\mu_B(\mu_B - 1) \\ + \; &k_p V_r\left(\mu_B^2\lambda_p + a_3 a_4\mathcal{R}_0^{(1)}\right) + V_r\beta_p[V_r\theta_r\lambda_r + \theta_p\lambda_r] + k_p\beta_r[\theta_p\lambda_p + V_r\theta_r(\lambda_p - 1)]\}.\end{aligned} \tag{A-5}$$

It should be noted from (A-5) that the right-hand side of the inequality is automatically negative (since all the parameters of the model are nonnegative). The left-hand side of the inequality (A-5) can be written as

$$a_3\left[a_4(a_3 + a_4) + \lambda_p(a_3 + a_4 + \lambda_p) + \lambda_p(\lambda_r + \mu_B - 1)\right]\left(1 - \mathcal{R}_0^{(1)}\right), \tag{A-6}$$

which is always positive whenever $\mathcal{R}_0^{(1)} < 1$ (noting that $\mu_B - 1 \geq 0$). Hence, the Routh-Hurwitz condition $b_1 b_2 - b_0 > 0$ always holds when $\mathcal{R}_0^{(1)} < 1$ (since the left-hand side of the inequality is always positive, and the right-hand side of the same inequality is always negative).

A2: Positivity of the Discriminant of Equation (3.16)

Recall that the discriminant of Equation (3.16) is given by:

$$\Delta_p = d_2^2 d_1^2 + 18 d_1 d_2 d_0 - 4 d_1^3 - 4 d_0 d_2^3 - 27 d_0^2, \tag{A-7}$$

with d_2, d_1 and d_0 as defined in Equation (3.17). The expression (A-7) (with (3.17)) can be simplified to:

$$\begin{aligned}
\Delta_p \;=\; & \frac{1}{a_3^3 k_p^3 V_r^3 \mu_B^4 (\lambda_p + a_4)^4} \{4\, a_3^2 k_p^3 V_r^3 \beta_r \theta_r a_4^3 + 4\mu_B(\lambda_p + a_4)[k_p \beta_r\, (\theta_p \lambda_p + V_r \theta_r (\lambda_p + \mu_B)) \\
+ \;& V_r \beta_p (V_r \theta_r \lambda_r + \theta_p (\lambda_r + \;\mu_B))]^3 + a_3 k_p V_r [V_r^2 \beta_p^2 a_4^2 (V_r \theta_r\, \lambda_r + \theta_p a_4)^2 \\
+ \;& 2 k_p V_r \beta_p \beta_r a_4 (V_r \theta_r \lambda_r + \theta_p a_4)(\theta_p \lambda_p a_4 + V_r \theta_r (10\mu_B a_4 + \lambda_p (\;\lambda_r + 10\mu_B))) \\
+ \;& k_p^2 \beta_r^2 [\theta_p^2 \lambda_p^2 a_4^2 + 2 V_r \theta_p \theta_r \lambda_p a_4\, (10\mu_B a_4 + \lambda_p(\lambda_r + 10\mu_B)) + V_r^2 \theta_r^2 (-8\mu_B^2 a_4^2 \\
+ \;& \lambda_p^2 (\lambda_r^2 + 20\lambda_r \mu_B - 8\mu_B^2) + 4\lambda_p \mu_B (5\lambda_r^2 + \lambda_r \mu_B - 4\mu_B^2)))]]\} > 0.
\end{aligned}$$

Appendix B

Theorem 7 in [39] can be used to obtain an ordering of the relationship between the associated basic reproduction numbers of the rescaled model (2.3) ($\mathcal{R}_0^{(i)};\ i = 1, ..., 4$). To do so, let J be the Jacobian matrix of the rescaled model (2.3). The matrix J can then be expressed in terms of the associated transmission matrices (F_i) and the transition matrices (V_i), with $i = 1, ..., 4$. That is, $J = F_1 - V_1 = F_2 - V_2 = F_3 - V_3 = F_4 - V_4$. Let $X = [x_{ij}]$ and $Y = [y_{ij}]$ be any two matrices. The inequality $X > Y$ means that $x_{ij} > y_{ij}$ for any i, j [39]. It can be seen from the matrices given by Equations (3.2), (3.7), (3.11), (3.14) that

$$F_1 \leq F_2 \leq F_4 \qquad \text{and } F_1 \leq F_3 \leq F_4. \tag{A-8}$$

Further, the matrices F_i and V_i ($i = 1, ..., 4$) are nonnegative and V_i^{-1} exist for any $i = 1, ..., 4$. Hence, it follows from Theorem 7 in [39], that partial ordering between $\mathcal{R}_0^{(1)}$, $\mathcal{R}_0^{(2)}$ and $\mathcal{R}_0^{(4)}$, and between $\mathcal{R}_0^{(1)}$, $\mathcal{R}_0^{(3)}$ and $\mathcal{R}_0^{(4)}$, exist. More specifically, one of the following relations holds [39]:

1. $1 < \mathcal{R}_0^{(4)} < \mathcal{R}_0^{(2)} < \mathcal{R}_0^{(1)}$ and $1 < \mathcal{R}_0^{(4)} < \mathcal{R}_0^{(3)} < \mathcal{R}_0^{(1)}$;
2. $\mathcal{R}_0^{(1)} = \mathcal{R}_0^{(2)} = \mathcal{R}_0^{(4)} = 1$ and $\mathcal{R}_0^{(1)} = \mathcal{R}_0^{(3)} = \mathcal{R}_0^{(4)} = 1$;
3. $\mathcal{R}_0^{(1)} < \mathcal{R}_0^{(2)} < \mathcal{R}_0^{(4)} < 1$ and $\mathcal{R}_0^{(1)} < \mathcal{R}_0^{(3)} < \mathcal{R}_0^{(4)} < 1$.

The matrices F_2 and F_3 are not comparable. Hence, no partial (inequality) ordering between $\mathcal{R}_0^{(2)}$ and $\mathcal{R}_0^{(3)}$ can be established using the theorem in [39] (except when both reproduction numbers are equal to unity). Combining the equations in Item 2 above reproduces the relation (3.20).

Appendix C: Proof of Theorem 4.3

Proof. Consider the normalized model (2.3) with $v_p(t)$ at its maximum value ($v_p(t) = 1$) for all t in $\mathcal{D}$. Further, let $\mathcal{R}_0^{(1)} = \left(\mathcal{R}_0^{(3)}\right)^2 \leq 1$. Consider the following Lyapunov function (noting that, since $\mu_B - 1 \geq 0$, all coefficients of the Lyapunov function are positive):

$$\mathcal{L}(i, b_p, b_r) = \mathcal{R}_0^{(3)} i + \frac{\beta_p a_4 V_r + \beta_r k_p \lambda_p}{k V_r [a_4(\mu_B - 1) + \lambda_p \mu_B]} b_p + \frac{\beta_p \lambda_r V_r + \beta_r k_p (\mu_B - 1 + \lambda_p)}{k_p [a_4(\mu_B - 1) + \lambda_p \mu_B]} b_r, \tag{B-1}$$

with Lyapunov derivative given by:

$$\begin{aligned}
\dot{\mathcal{L}} &= \mathcal{R}_0^{(3)} \dot{i} + \frac{\beta_p a_4 V_r + \beta_r k_p \lambda_p}{k_p V_r [a_4(\mu_B - 1) + \lambda_p \mu_B]} \dot{b}_p + \frac{\beta_p \lambda_r V_r + \beta_r k_p (\mu_B - 1 + \lambda_p)}{k_p [a_4(\mu_B - 1) + \lambda_p \mu_B]} \dot{b}_r \\
&= \mathcal{R}_0^{(3)} \left[\left(\frac{\beta_p}{k_p + b_p} b_p + \frac{\beta_r}{1 + b_r} b_r \right) s - a_3 i \right] \\
&+ a_3 \frac{\left(\mathcal{R}_0^{(3)}\right)^2 (\beta_p a_4 V_r + \beta_r k_p \lambda_p)}{V_r \beta_p a_1 + k_p \beta_r \left[(\theta_p + V_r \theta_r) \lambda_p + V_r \theta_r (\mu_B - 1) \right]} \left[\theta_p i + b_p (1 - b_p) - \mu_B b_p + \lambda_r V_r b_r - \lambda_p b_p \right] \\
&+ a_3 \frac{V_r \left(\mathcal{R}_0^{(3)}\right)^2 (\beta_p \lambda_r V_r + \beta_r k_p (\mu_B - 1 + \lambda_p))}{V_r \beta_p a_1 + k_p \beta_r \left[(\theta_p + V_r \theta_r) \lambda_p + V_r \theta_r (\mu_B - 1) \right]} \left[\theta_r i - \mu_B b_r - \lambda_r b_r + \lambda_p \frac{b_p}{V_r} \right] \\
&= a_3 (\mathcal{R}_0^{(3)} - 1) \left(\mathcal{R}_0^{(3)} i + \frac{\beta_p b_p}{k_p a_3} + \frac{\beta_r b_r}{a_3} \right) \\
&- \mathcal{R}_0^{(3)} \left[\frac{\beta_p b_p}{k_p} \left(1 - \frac{k_p s}{k_p + b_p} \right) + \beta_r b_r \left(1 - \frac{s}{1 + b_r} \right) \right] \\
&- \frac{a_3 \left(\mathcal{R}_0^{(3)}\right)^2 (\beta_p a_4 V_r + \beta_r k_p \lambda_p)}{V_r \beta_p a_1 + k_p \beta_r \left[(\theta_p + V_r \theta_r) \lambda_p + V_r \theta_r (\mu_B - 1) \right]} b_p^2.
\end{aligned} \tag{B-2}$$

Since $s(t) \leq 1$ for all $t > 0$ in $\mathcal{D}$, it follows from (B-2) that $\frac{k_p s}{k_p + b_p} \leq 1$ and $\frac{s}{1 + b_r} \leq 1$. Hence,

$$\dot{\mathcal{L}} \leq (\mathcal{R}_0^{(3)} - 1) \left(\mathcal{R}_0^{(3)} i + \frac{\beta_p}{k_p a_3} b_p + \frac{\beta_r}{a_3} b_r \right). \tag{B-3}$$

It follows from (B-3) that $\dot{\mathcal{L}} < 1$ whenever $\mathcal{R}_0^{(3)} < 1$. Furthermore, it follows from (B-2) and (B-3) that $\dot{\mathcal{L}} = 0$ if and only if:

(a) $\mathcal{R}_0^{(3)} = 1$ and $s(t) = 1$, or

(b) $i(t) = b_p(t) = b_r(t) = 0$.

In either of the above two cases, the largest compact invariant subset of the set

$$\mathcal{G} = \{(s, i, b_p, b_r, v_p) \in \mathcal{D} : \dot{\mathcal{L}} = 0\}$$

is the singleton $\{\mathbf{E}_0\}$. In fact, suppose $\mathcal{M}$ is the largest compact invariant subset of $\mathcal{G}$. To check for Case (a), we need to require that $s(t) = 1$ is the solution of the human component of the normalized model given

by:

$$\begin{cases} \dot{s} = \mu(1-s) - \left(\frac{\beta_p b_p}{k_p+b_p} + \frac{\beta_r b_r}{1+b_r}\right) s + \gamma i, \\ \dot{i} = \left(\frac{\beta_p b_p}{k_p+b_p} + \frac{\beta_r b_r}{1+b_r}\right) s - a_3 i, \end{cases} \tag{B-4}$$

from which it follows (by adding the two equations, and recalling that $n(t) = s(t) + i(t)$)) that:

$$\dot{n} = \mu(1-s) - (\delta+\mu)i. \tag{B-5}$$

Substituting $s(t) = 1$ in (B-5) (and noting that, for solution of the form $s(t) = 1$, $\dot{s} = 0$) gives:

$$\dot{i} = -(\delta+\mu)i, \tag{B-6}$$

so that $\lim_{t\to\infty} i(t) = 0$. Substituting $s(t) = 1$ and $i(t) = 0$ into the normalized model (2.3) shows that $\lim_{t\to\infty} (b_p(t), b_r(t)) = (0,0)$. Hence, it follows from the above analyses that, for Case (a), $\lim_{t\to 0}(s(t), i(t), b_p(t), b_r(t)) = (1,0,0,0)$. Thus, for Case (a), $\mathcal{M} = \{\mathbf{E}_0\}$ and all solutions in $\mathcal{D}$ converge to the disease-free equilibrium ($\mathbf{E}_0$) of the normalized model.

Similarly, for Case (b), requiring each solution in $\mathcal{M}$ to satisfy $i(t) = b_p(t) = b_r(t) = 0$ leads to:

$$\dot{s} = \mu(1-s), \tag{B-7}$$

whose solution is (where $s_0 = s(0) > 0$ and $0 < s_0 \leq 1$)

$$s(t) = 1 - (1-s_0)\, e^{-\mu t}. \tag{B-8}$$

Since $\mu > 0$ and $0 < s_0 \leq 1$, it follows from (B-8) that $\lim_{t\to\infty} s(t) = 1$. That is, in Case (b) (where $i(t) = b_p(t) = b_r(t) = 0$), like in Case (a), the largest compact invariant subset where $\dot{\mathcal{L}} = 0$ is the singleton $\{\mathbf{E}_0\}$. Thus, it follows from the LaSalle's Invariance Principle [37] that the disease-free equilibrium of the normalized model ($\{\mathbf{E}_0\}$) is globally-asymptotically stable in $\mathcal{D}$ whenever $\mathcal{R}_0^{(3)} \leq 1$. □

It is worth mentioning that the above proof also works for the special case where $v_p(t) \neq 1$, if the associated water balance condition, $k_p \leq \frac{b_p(t)}{1-v_p(t)}$, holds (for all time $t \geq 0$).

References

[1] M. Ali, A. R. Nelson, A. L. Lopez, and D. A. Sack. Updated global burden of cholera in endemic countries. *PLoS Neglected Tropical Diseases*, 9(6):e0003832, 2015.

[2] R. M. Anderson and R. M. May. Population biology of infectious diseases: Part i. *Nature*, 280(5721):361, 1979.

[3] G. A.J. Ayliffe, B.J. Collins, L. J. Taylor, et al. *Hospital-acquired infection: principles and prevention.* Bristol, UK; John Wright & Sons Ltd., 1982.

[4] W.B. Baine, M. Mazzotti, D. Greco, E. Izzo, A. Zampieri, G. Angioni, M. Di Gioia, E.J. Gangarosa, and F. Pocchiari. Epidemiology of cholera in italy in 1973. *The Lancet*, 304(7893):1370–1374, 1974.

[5] M. Bani-Yaghoub, R. Gautam, Z. Shuai, P. Van Den Driessche, and R. Ivanek. Reproduction numbers for infections with free-living pathogens growing in the environment. *Journal of Biological Dynamics*, 6(2):923–940, 2012.

[6] S. Barve, T.B. Javadekar, S. Nanda, C. Pandya, A. Pathan, and P. Chavda. Isolation of vibrio cholera o1 during an outbreak of acute gastroenteritis in dahod district, gujarat. *Nat J Community Med*, 3:104–7, 2012.

[7] E. Bertuzzo, S. Azaele, A. Maritan, M. Gatto, I. Rodriguez-Iturbe, and A. Rinaldo. On the space-time evolution of a cholera epidemic. *Water Resources Research*, 44(1), 2008.

[8] E. Bertuzzo, R. Casagrandi, M. Gatto, I. Rodriguez-Iturbe, and A. Rinaldo. On spatially explicit models of cholera epidemics. *Journal of the Royal Society Interface*, 7(43):321–333, 2009.

[9] E. Bertuzzo, L. Mari, L. Righetto, M. Gatto, R. Casagrandi, M. Blokesch, I. Rodriguez-Iturbe, and A. Rinaldo. Prediction of the spatial evolution and effects of control measures for the unfolding Haiti cholera outbreak. *Geophysical Research Letters*, 38(6), 2011.

[10] E. Bertuzzo, L. Mari, L. Righetto, M. Gatto, R. Casagrandi, I. Rodriguez-Iturbe, and A. Rinaldo. Hydroclimatology of dual-peak annual cholera incidence: insights from a spatially explicit model. *Geophysical Research Letters*, 39(5), 2012.

[11] L. Bourouiba, A. Teslya, and J. Wu. Highly pathogenic avian influenza outbreak mitigated by seasonal low pathogenic strains: Insights from dynamic modeling. *Journal of Theoretical Biology*, 271(1):181–201, 2011.

[12] J. M Boyce, G. Potter-Bynoe, C. Chenevert, and T. King. Environmental contamination due to methicillin-resistant Staphylococcus aureus possible infection control implications. *Infection Control & Hospital Epidemiology*, 18(9):622–627, 1997.

[13] V. Capasso and S.L. Paveri-Fontana. A mathematical model for the 1973 cholera epidemic in the european mediterranean region. *Revue d'épidémiologie et de Santé Publiqué*, 27(2):121–132, 1979.

[14] P. P. Chapagain, J.S. Van Kessel, J.S. Karns, D.R. Wolfgang, E. Hovingh, K.A. Nelen, Y.H. Schukken, and Y.T. Grohn. A mathematical model of the dynamics of salmonella cerro infection in a us dairy herd. *Epidemiology & Infection*, 136(2):263–272, 2008.

[15] M. Ciddio. Sviluppo di un modello spazialmente esplicito di diffusione del colera e sua applicazione al caso endemico del Bangladesh. *Thesis*, 2012.

[16] C. T. Codeço. Endemic and epidemic dynamics of cholera: the role of the aquatic reservoir. *BMC Infectious Diseases*, 1(1):1, 2001.

[17] R. R Colwell and A. Huq. Environmental reservoir of vibrio cholerae the causative agent of cholera. *Annals of the New York Academy of Sciences*, 740(1):44–54, 1994.

[18] R. R Colwell, J. Kaper, and S.W. Joseph. Vibrio cholerae, vibrio parahaemolyticus, and other vibrios: occurrence and distribution in chesapeake bay. *Science*, 198(4315):394–396, 1977.

[19] A. Cozad and R. D. Jones. Disinfection and the prevention of infectious disease. *American Journal of Infection Control*, 31(4):243–254, 2003.

[20] D. Danforth, L.E. Nicolle, K. Hume, N. Alfieri, and H. Sims. Nosocomial infections on nursing units with floors cleaned with a disinfectant compared with detergent. *Journal of Hospital Infection*, 10(3):229–235, 1987.

[21] F. Daschner and A. Schuster. Disinfection and the prevention of infectious disease: No adverse effects? *American Journal of Infection Control*, 32(4):224–225, 2004.

[22] O. Diekmann and J. A. P. Heesterbeek. *Mathematical epidemiology of infectious diseases: model building, analysis and interpretation*, volume 5. John Wiley & Sons, 2000.

[23] O. Diekmann, J. A. P. Heesterbeek, and J. A.J. Metz. On the definition and the computation of the basic reproduction ratio R_0 in models for infectious diseases in heterogeneous populations. *Journal of Mathematical Biology*, 28(4):365–382, 1990.

[24] M. C. Eisenberg, S. L. Robertson, and J. H. Tien. Identifiability and estimation of multiple transmission pathways in cholera and waterborne disease. *Journal of Theoretical Biology*, 324:84–102, 2013.

[25] R. Feachem, D. D. Mara, and D.J. Bradley. *Sanitation and disease*. John Wiley & Sons Washington DC, USA:, 1983.

[26] I. C.H. Fung, D. L. Fitter, R. H. Borse, M. I. Meltzer, and J. W. Tappero. Modeling the effect of water, sanitation, and hygiene and oral cholera vaccine implementation in haiti. *The American Journal of Tropical Medicine and Hygiene*, 89(4):633–640, 2013.

[27] N. H. Gaffga, R. V. Tauxe, and E. D. Mintz. Cholera: a new homeland in africa? *The American Journal of Tropical Medicine and Hygiene*, 77(4):705–713, 2007.

[28] K.T. Goh, S.H. Teo, S. Lam, and M.K. Ling. Person-to-person transmission of cholera in a psychiatric hospital. *Journal of Infection*, 20(3):193–200, 1990.

[29] D. M. Hartley, J. G. Morris Jr., and D. L. Smith. Hyperinfectivity: a critical element in the ability of V. cholerae to cause epidemics? *PLoS Medicine*, 3(1):e7, 2005.

[30] J.A.P. Heesterbeek and M.G. Roberts. The type-reproduction number t in models for infectious disease control. *Mathematical Biosciences*, 206(1):3–10, 2007.

[31] H. W. Hethcote. The mathematics of infectious diseases. *SIAM Review*, 42(4):599–653, 2000.

[32] L. K. Jackson and K. W. Schrader. Comparison theorems for nonlinear differential equations. *Journal of Differential Equations*, 3(2):248–255, 1967.

[33] M. A. Jensen, S. M. Faruque, J. J. Mekalanos, and B. R. Levin. Modeling the role of bacteriophage in the control of cholera outbreaks. *Proceedings of the National Academy of Sciences*, 103(12):4652–4657, 2006.

[34] W. Just, J. Saldaña, and Y. Xin. Oscillations in epidemic models with spread of awareness. *Journal of Mathematical Biology*, 76(4):1027–1057, 2018.

[35] M. Kitaoka, S. T. Miyata, D. Unterweger, and S. Pukatzki. Antibiotic resistance mechanisms of Vibrio cholerae. *Journal of Medical Microbiology*, 60(4):397–407, 2011.

[36] B.V.S. Krishna, A.B. Patil, and M.R. Chandrasekhar. Fluoroquinolone-resistant vibrio cholerae isolated during a cholera outbreak in india. *Transactions of the Royal Society of Tropical Medicine and Hygiene*, 100(3):224–226, 2006.

[37] J. P. LaSalle. *The stability of dynamical systems*, volume 25. Siam, 1976.

[38] S. A. Levin. Descartes' rule of signs - how hard can it be? 2002.

[39] M.A. Lewis, Z. Shuai, and P. van den Driessche. A general theory for target reproduction numbers with applications to ecology and epidemiology. *Journal of Mathematical Biology*, 78(7):2317–2339, 2019.

[40] D. G. Maki, C. J. Alvarado, C. A. Hassemer, and M. A. Zilz. Relation of the inanimate hospital environment to endemic nosocomial infection. *New England Journal of Medicine*, 307(25):1562–1566, 1982.

[41] L. Mari, E. Bertuzzo, L. Righetto, R. Casagrandi, M. Gatto, I. Rodriguez-Iturbe, and A. Rinaldo. Modelling cholera epidemics: the role of waterways, human mobility and sanitation. *Journal of the Royal Society Interface*, 9(67):376–388, 2011.

[42] Z. Mukandavire, S. Liao, J. Wang, H. Gaff, D. L. Smith, and J. G. Morris. Estimating the reproductive numbers for the 2008–2009 cholera outbreaks in zimbabwe. *Proceedings of the National Academy of Sciences*, 108(21):8767–8772, 2011.

[43] R. Mukherjee, D. Halder, S. Saha, R. Shyamali, C. Subhranshu, R. Ramakrishnan, M. V. Murhekar, and Y. J. Hutin. Five pond-centred outbreaks of cholera in villages of west bengal, india: evidence for focused interventions. *Journal of Health, Population, and Nutrition*, 29(5):421, 2011.

[44] World Health Organization. African Health Ministers Commit to Ending Cholera Outbreaks by 2030. website: https://www.afro.who.int/news/african-health-ministers-commit-ending-cholera-outbreaks-2030. accessed: March 2019.

[45] World Health Organization. Cholera: Key Facts, 2019. webpage: https://www.who.int/news-room/fact-sheets/detail/cholera (accessed march 2019).

[46] World Health Organization. Global task force on cholera control webpage: https://www.who.int/cholera/publications/global-roadmap.pdf (accessed june 2019).

[47] World Health Organization. Largest Cholera Vaccine Drive in History to Target Spike in Outbreaks. 2018. website: https://www.who.int/news-room/detail/07-05-2018-largest-cholera-vaccine-drive-in-history-to-target-spike-in-outbreaks. accessed: March 2019.

[48] World Health Organization. THE TREATMENT OF DIARRHOEA, A manual for physicians and other senior health workers webpage: https://www.who.int/news-room/fact-sheets/detail/cholera (archived 2011-10-19 at the wayback machine), 2005, chapter 5: "management of suspected cholera".

[49] M. Pascual, M. J. Bouma, and A. P. Dobson. Cholera and climate: revisiting the quantitative evidence. *Microbes and Infection*, 4(2):237–245, 2002.

[50] Z. Rahman, M. Rahman, M. Rashid, S. Monira, F.T. Johura, M. Mustafiz, S. I. Bhuyian, F. Zohura, T. Parvin, K. Hasan, et al. Vibrio cholerae Transmits through Water among the Household Contacts of Cholera Patients in Cholera Endemic Coastal Villages of Bangladesh, 2015-2016 (CHoBI7 Trial). *Frontiers in Public Health*, 6:238, 2018.

[51] L. Righetto, R. Casagrandi, E. Bertuzzo, L. Mari, M. Gatto, I. Rodriguez-Iturbe, and A. Rinaldo. The role of aquatic reservoir fluctuations in long-term cholera patterns. *Epidemics*, 4(1):33–42, 2012.

[52] M.G. Roberts and J.A.P. Heesterbeek. A new method for estimating the effort required to control an infectious disease. *Proceedings of the Royal Society of London. Series B: Biological Sciences*, 270(1522):1359–1364, 2003.

[53] D. A. Sack, R.B. Sack, B. Nair, and A.K. Siddique. Cholera. *The Lancet*, 363, 2004.

[54] D.A. Sack, R.B. Sack, and L.C. Chaignat. Getting serious about cholera. *The New England Journal of Medicine*, 355(7):649, 2006.

[55] M. A. Safi, D. Y. Melesse, and A. B. Gumel. Dynamics analysis of a multi-strain cholera model with an imperfect vaccine. *Bulletin of Mathematical Biology*, 75(7):1104–1137, 2013.

[56] R. P. Sanches, C. P. Ferreira, and R. A. Kraenkel. The role of immunity and seasonality in cholera epidemics. *Bulletin of Mathematical Biology*, 73(12):2916–2931, 2011.

[57] E. Scott and S. F. Bloomfield. The survival and transfer of microbial contamination via cloths, hands and utensils. *Journal of Applied Bacteriology*, 68(3):271–278, 1990.

[58] Z. Shuai, J.A.P. Heesterbeek, and P. van Den Driessche. Extending the type reproduction number to infectious disease control targeting contacts between types. *Journal of Mathematical Biology*, 67(5):1067–1082, 2013.

[59] Z. Shuai, J.A.P. Heesterbeek, and P. van den Driessche. Erratum to: Extending the type reproduction number to infectious disease control targeting contacts between types. *Journal of Mathematical Biology*, 71(1):255–257, 2015.

[60] A.K. Siddique, K. Zaman, A.H. Baqui, K. Akram, P. Mutsuddy, A. Eusof, K. Haider, S. Islam, and R.B. Sack. Cholera epidemics in Bangladesh: 1985-1991. *Journal of Diarrhoeal Diseases Research*, pages 79–86, 1992.

[61] W.M. Spira, M. U. Khan, Y.A. Saeed, and M.A. Sattar. Microbiological surveillance of intra-neighbourhood El Tor cholera transmission in rural Bangaldesh. *Bulletin of the World Health Organization*, 58(5):731, 1980.

[62] THEENDFUND. Schistosomiasis. webpage: https://end.org/ntds-in-focus/schistosomiasis/ (accessed july 2018).

[63] J. H. Tien and D. J.D. Earn. Multiple transmission pathways and disease dynamics in a waterborne pathogen model. *Bulletin of Mathematical Biology*, 72(6):1506–1533, 2010.

[64] The New York Times. Poor Sanitation Persisted at U.N. Missions Long After Haiti Cholera Crisis. webpage: https://www.nytimes.com/2016/08/20/world/americas/haiti-cholera-sanitation-un-peacekeepers.html (accessed may 2019).

[65] H.W. Turnbull. *THEORY OF EQUATIONS*. OLIVER AND BOYD, 1947.

[66] P. Van den Driessche and J. Watmough. Reproduction numbers and sub-threshold endemic equilibria for compartmental models of disease transmission. *Mathematical Biosciences*, 180(1-2), 2002.

[67] R. A Weinstein and B. Hota. Contamination, disinfection, and cross-colonization: are hospital surfaces reservoirs for nosocomial infection? *Clinical Infectious Diseases*, 39(8):1182–1189, 2004.

[68] Wikipedia. Cholera. accessed: May 2019. webpaege https://en.wikipedia.org/wiki/cholera.

[69] J. N. Zuckerman, L. Rombo, and A. Fisch. The true burden and risk of cholera: implications for prevention and control. *The Lancet Infectious Diseases*, 7(8):521–530, 2007.